REPORT DOCUMENTATION PAGE

Form Approved
OMB No. 0704-0188

AD-A267 150

2. REPORT DATE	3. REPORT TYPE AND DATES COVERED
June 20, 1993	Final Report 8/89-2/93

4. TITLE AND SUBTITLE
Laser Assisted CVD Growth of AlN and GaN

5. FUNDING NUMBERS
F49620-89-C-0108
Proc. Inst No.
F08671-89-01458 2306/
Bl Req. No.

6. AUTHOR(S)
Dr. Joshua B. Halpern
Dr. Joan M. Frye

7. PERFORMING ORGANIZATION NAME(S) AND ADDRESS(ES)
Department of Chemistry and
Materials Science Research Center of Excellence
Howard University
Washington, DC 20059

8. PERFORMING ORGANIZATION REPORT NUMBER
AFOSR-TR- [illegible] 8

9. SPONSORING/MONITORING AGENCY NAME(S) AND ADDRESS(ES)
USAF/AFSC
AirForce Office of Scientific Research
Building 410
Bolling AFB, DC 20332-6448

10. SPONSORING/MONITORING AGENCY REPORT NUMBER
F4920-89-C-0103

11. SUPPLEMENTARY NOTES

12a. DISTRIBUTION/AVAILABILITY STATEMENT
Unlimited

12b. DISTRIBUTION CODE

13. ABSTRACT (Maximum 200 words)

This is the final report of a project for investigating laser (assisted) methods of growing nitrile thin films. We have grown thin films of AlN and SiN by laser ablation from powders. We have also developed an efficient method for laser assisted CVD of aluminum, or aluminum containing films from trimethylaluminum.

Codes
Dist | Avail and/or Special
A-1

93-16890

14. SUBJECT TER

15. NUMBER OF PAGES

16. PRICE CODE

17. SECURITY CLASSIFICATION OF REPORT	18. SECURITY CLASSIFICATION OF THIS PAGE	19. SECURITY CLASSIFICATION OF ABSTRACT	20. LIMITATION OF ABSTRACT
Unclassified	Unclassified	Unclassified	None

1.0 Introduction

The goal of this project was to design, test and verify advanced processes using lasers for the growth of nitride semiconductor materials. Papers have been published on:

a: Pulsed laser deposition of silicon nitride. Proceedings of the Materials Research Society, 285 (1993) 331.

b: Rapid growth of AlN thin films by pulsed laser deposition. Applied Physics Letters 60 (1992) 2234.

c: Wavelength dependence of the deposition of Al (and by implication Al in any compound semiconductor such as AlN). Journal of Crystal Growth, (1993) in proof.

In addition this work has resulted in a Master Thesis in Electrical Engineering: Pulsed Laser Deposition of Aluminum Nitride and Silicon Nitride Thin Films. Xiangqun Xu, Howard University, May 1993.

Moreover, work has been done on:

d. Pulsed laser deposition combined with remote plasma nitration, which substantially increases the amount of nitrogen in the binary semiconductors.

In particular, we are continuing to work on item d, which is the most promising process of those we have investigated for growth of nitrides thin film.

2.0 Pulsed Laser Deposition of Silicon Nitride

Silicon nitride thin films are used as dielectric materials and for functional memory layers in microelectronic and optoelectronic devices [2.1-5]. The standard methods for deposition are CVD [2.1], plasma enhanced CVD [2.2] and direct thermal nitration [2.3]. We

have grown silicon nitride thin films by PLD and by remote plasma enhanced PLD. These methods have the advantage of exposing the substrate to a less hostile environment than the other methods. For example CVD requires temperatures above 600 C, while plasma enhanced CVD operates at lower thermal temperatures (300 C) but places the substrate in an environment filled with high energy ions and electrons.

2.1 PLD of Silicon Nitride from Si_3N_4 Powder

2.1.1 Methodology

A 13mm diameter target pellet was prepared from electronic grade Si_3N_4 powder obtained from Johnson and Mathey using a 2.5 ton/cm^2 hydraulic press. The pellet was placed in a high vacuum system. parallel to the substrate and at 45^o to the laser beam. Films were grown on Si (100) wafers, KBr and Supracil quartz plates. We used light from both 248 nm KrF and 193 nm ArF lasers with a 20 ns pulse width focussed on the powder tablet with a 160 mm focal length lens. In general, this soft focus, produced a better film than using a tight focus. The fluence at the target we between 1 and 6 J/cm^2. The substrate was mounted on a stage which could be heated to over 300 C. The vacuum chamber was evacuated by a 4" diffusion pump and a liquid nitrogen trap stopped backstreaming. Films were characterized by Auger, IR and UV spectroscopy, as well optical microscopy. Film thickness was measured by a depth profilometer.

2.1.2 Growth rate and film stoichiometry

Auger spectroscopy was used to determine the Si/N ratio in the deposited films as a function of substrate temperature. The films were found to be hydrogen free. Maintaining a relatively high vacuum (> 10^{-4} Torr) is necessary to eliminate oxygen contamination. The results are shown in Figure 2.1. As can be seen the stoichilmetric quality of the film improves as the temperature of the substrate is raised.

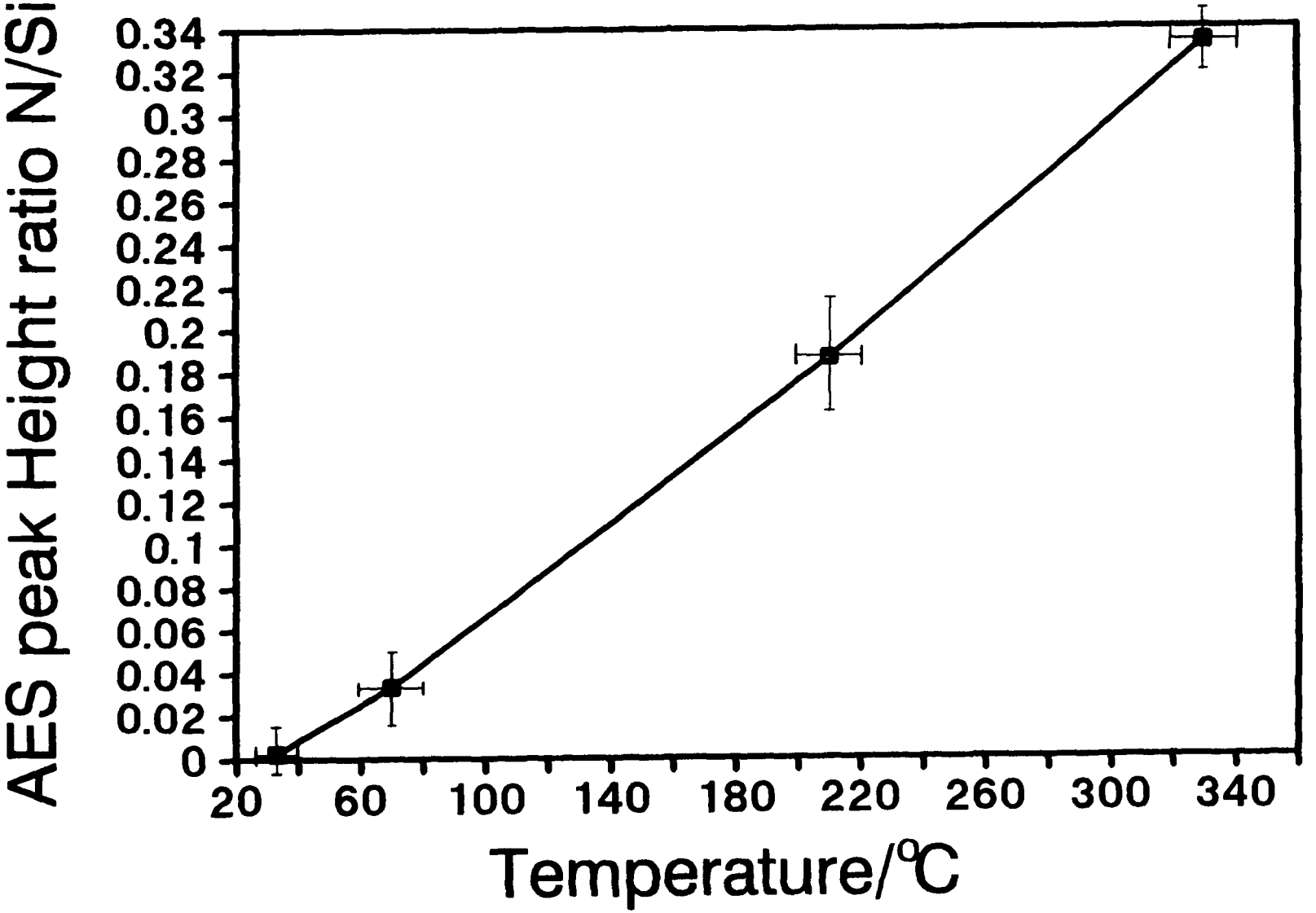
AES peak Height ratio N/Si
0.34
0.32
0.3
0.28
0.26
0.24
0.22
0.2
0.18
0.16
0.14
0.12
0.1
0.08
0.06
0.04
0.02
0
20
60
100
140
180
220
260
300
340
Temperature/°C

Figure 2.2 shows a study of film thickness vs. substrate temperature after 18,000 shots at a fluence of 6J/cm^2. Growth rates as high as 0.2 nm/pulse could be obtained. This is extremely rapid as compared to other methods for growth of silicon nitride films. Figure 2.1 and 2.2 indicate that there may be a rate competition, between the deposition process and a heterogeneous process on the film in which physically absorbed or Si atoms with dangling bonds are removed from the surface. The increase in the N/Si ratio as the overall film growth rate decreases point to such a mechanism. We expect that the deposition rate is constant with resepect to substrate temperature since it is controlled by the laser desorption process, remote from the substrate while the desorption rate should increase with the temperature of the substrate.

Under these assumptions we can estimate the activation energy of the second process as the equivalent of about 100 cm^{-1} from the observed decrease in the growth rate. This is a reasonable value for a physically absorbed species. As a consequence, since even at room temperature, an average of 200 cm^{-1} is available, we might be able to improve the N/Si ratio simply by decreasing the laser pulse rate, providing additional time for pysically adsorbed Si atoms to desorb. Another method of accomplishing the same end would be to illuminate the growing thin film with a small portion of the excimer laser beam (6.2 eV photons), or preferably with another laser, such as a doubled Nd-YAG laser (532 nm) where the photons would only have enough energy to break weaker bonds.

We further verified the chemical composition of the thin films by growing a film on a KBr substrate. While films grown at room temperature showed absorption in the Si-O_2 antistretching mode region, as seen in Figure 2.3, films grown at higher temperatures clearly showed a shift to the 830 to 850 cm^{-1} region, characteristic of Si-N stretching modes.

We also measured the band gap of the SiN thin films by measuring the UV spectrum of films grown on Suprasil quartz substrates. Since the absorption coefficient α is given by

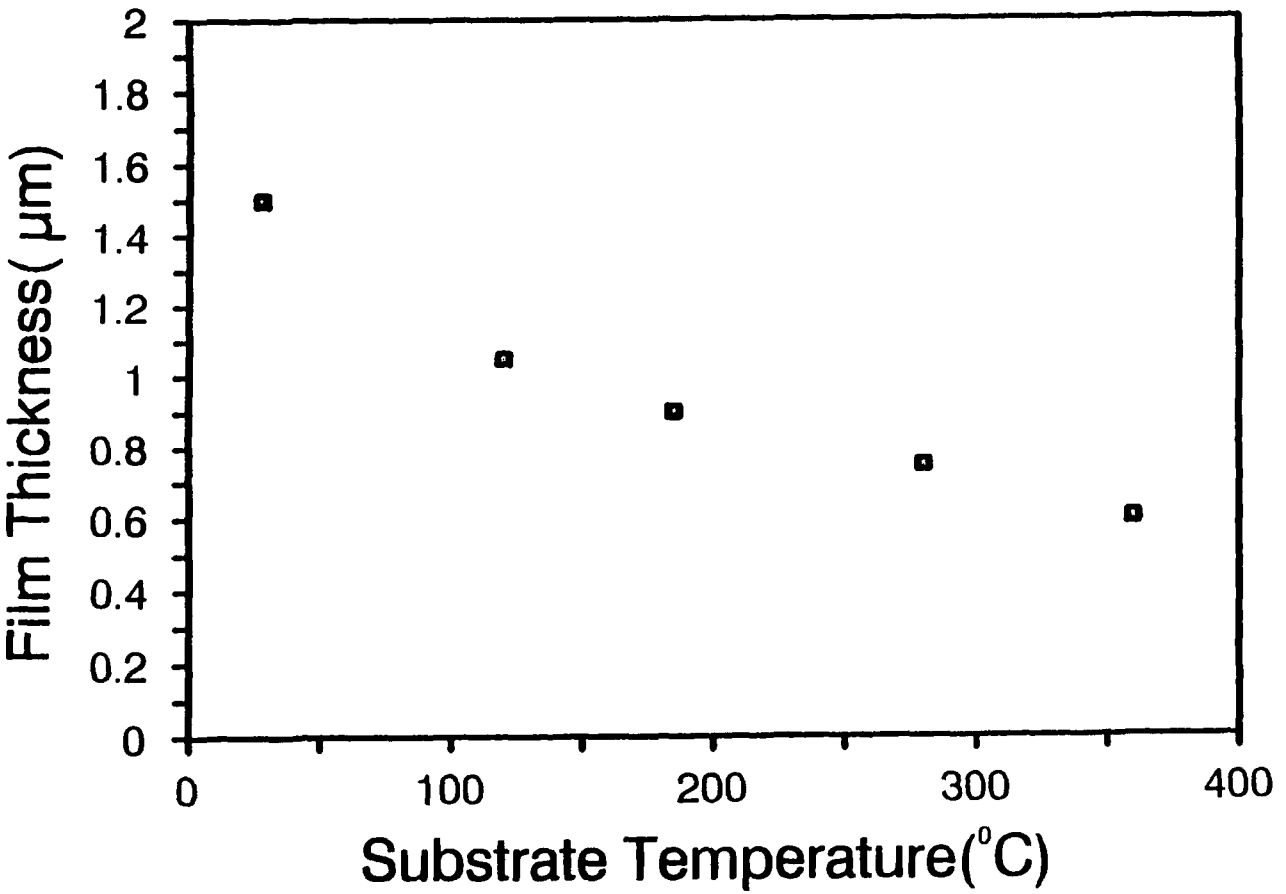

Relation between Si_3N_4 film thickness and substrate temperature after 15 min deposition with laser fluence of 6 J/cm² and a repetition rate of 5 Hz.

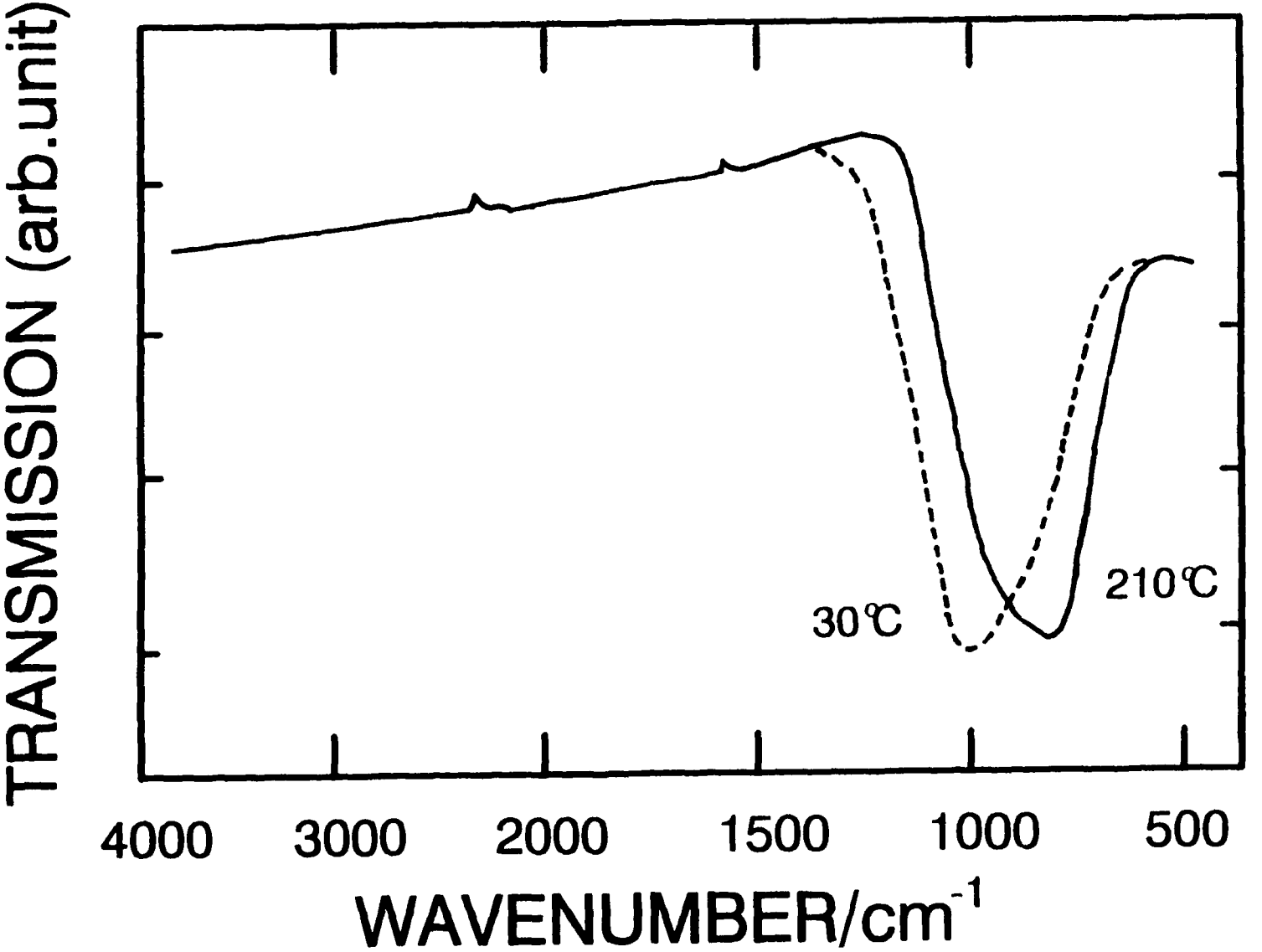
TRANSMISSION (arb.unit)
30℃
210℃
4000
3000
2000
1500
1000
500
WAVENUMBER/cm-1

(2.1) $$\alpha = [h\nu - E_g]^{1/2} h\nu$$

the energy gap, E_g, can be obtained by linear regression of $(h\nu\alpha)^2$ vs $h\nu$ as is shown in Figure 2.4. For a $SiN_{0.33}$ film the band gap is 5.60 eV. The non-linear behavior in the low energy region is due to scattering of the light by the surface. This is smaller than the 6.49 eV obtained by calculation [2.6] and is most likely due to the non-stoichiometric, silicon rich, nature of the film. The extra silicon also produces a subgap shoulder, which for amorphous silicon has been ascribed to dangling bonds (trivalent silicon atoms), however, this absorption is two orders of magnitude higher for the silicon nitride films [2.7].

Under a microscope, the films appeared smooth over a 1 to 4 cm^2 area. The splashing effect, characteristic of PLD was also seen, although one could eliminate this by velocity filtering, or overlapping of multiple focal sites on the target. There is a small velocity filtering effect caused by the geometric alaignment of the apparatus. Material projected at π /2 to the laser beam (along the direction of the plasma plume) is the most energetic and the highest velocity material. This is also the direction of the maximum material flux flow. The high energy is a result of plasma heating by the trailing edge of the laser pulse. Obversely, material ejected at 0 or π to the surface will be the slowest. Although the flux may be low in this direction, collisions with the thin film substrate will be relatively low energy and may be effective.

2.2. PLD of Silicon Nitride with Remote Plasma Nitration

While experience with other ceramic materials might lead one to believe that the target stoichiometry will be preserved during PLD, our experience with the nitrides and other work [2.8] has shown otherwise. The usual model is that the heating and cooling of the laser produced plasma takes place over times that are short compared to thermal diffusion and that the individual components cannot segregate.

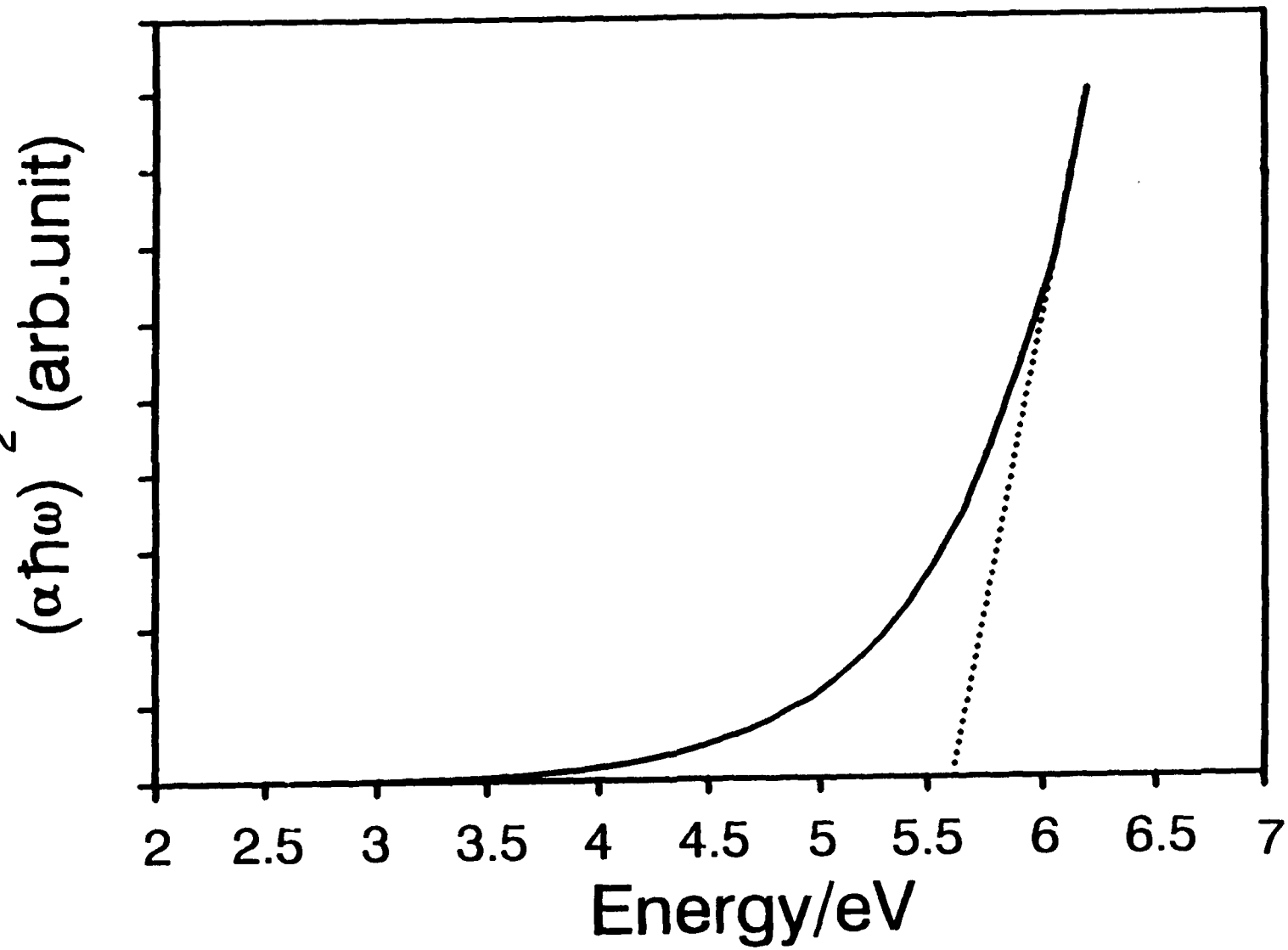
$(\alpha\hbar\omega)^2$ (arb.unit)
2
2.5
3
3.5
4
4.5
5
5.5
6
6.5
7
Energy/eV

There are two possible causes for the nitrogen poor nature of our films. First, N atom recombination in the plasma may be significant. The over 12 eV bond strength of diatomic nitrogen, would allow formation of molecules by third body recombination even in a very hot plasma. The stable nitrogen molecules would then be unavailable for film formation, resulting in nitrogen poor films. Second, N atoms may have a low sticking coefficient on the substrate due to either physical or chemical processes.

In either case, it should be possible to increase the N atom content of the films by providing an additional N atom source. The most straightforward method is to set up a remote plasma (microwave) discharge in nitrogen. Figure 2.5 shows how this was done. As a proof of concept a pure silicon wafer was used as the PLD target. Samples were grown with nitrogen gas pressures ranging from 80 to 400 mTorr and using microwave powers between 50 and 100 Watts. The discharge was excited in a 12 mm diameter glass tube surrounded by a tuned Evanson cavity. The tube was connected with our 6" cross growth chamber. Experience showed that the tube should be kept as short as possible to limit recombination. Substrate temperatures were varied between 200 and 450 C.

Figure 2.6 is an Auger survey of a deposited film, showing a significant N atom content from the remote plasma. We have also been able to increase the N atom content of films grown from SiN tablets. The O atom inclusion, is due either to residual oxygen in the chamber or (more likely) to a minescule oxygen molecule content of the nitrogen gas (99.999% nitrogen gas was used). Ammonia might prove better as a feed gas for this process, although hydrogen inclusion is not to be excluded in that case. Moreover, the ammonia itself, NH and NH_2 radicals and H atoms produced in such a discharge are reducing species, which would probably eliminate any oxidation of the thin films.

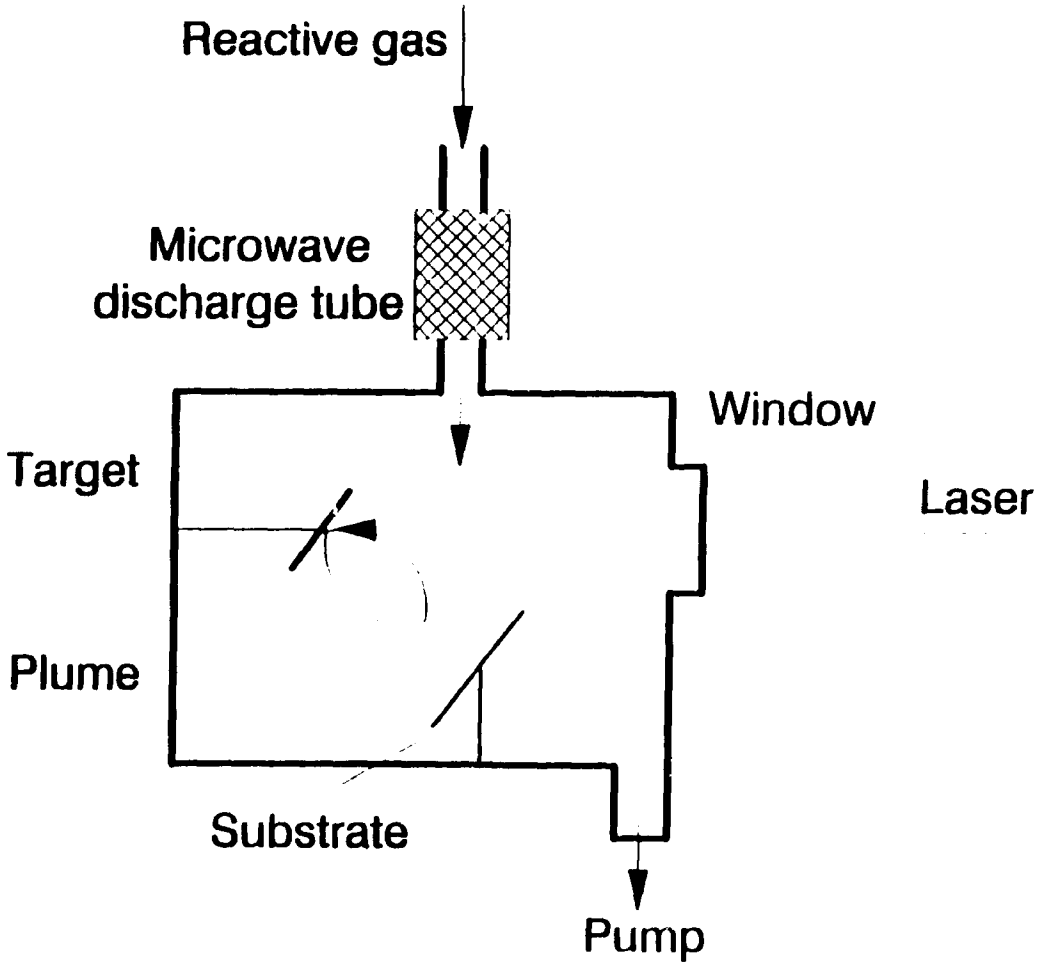

Schematic diagram of the microwave discharge set used up for nitride growth

AES SURVEY

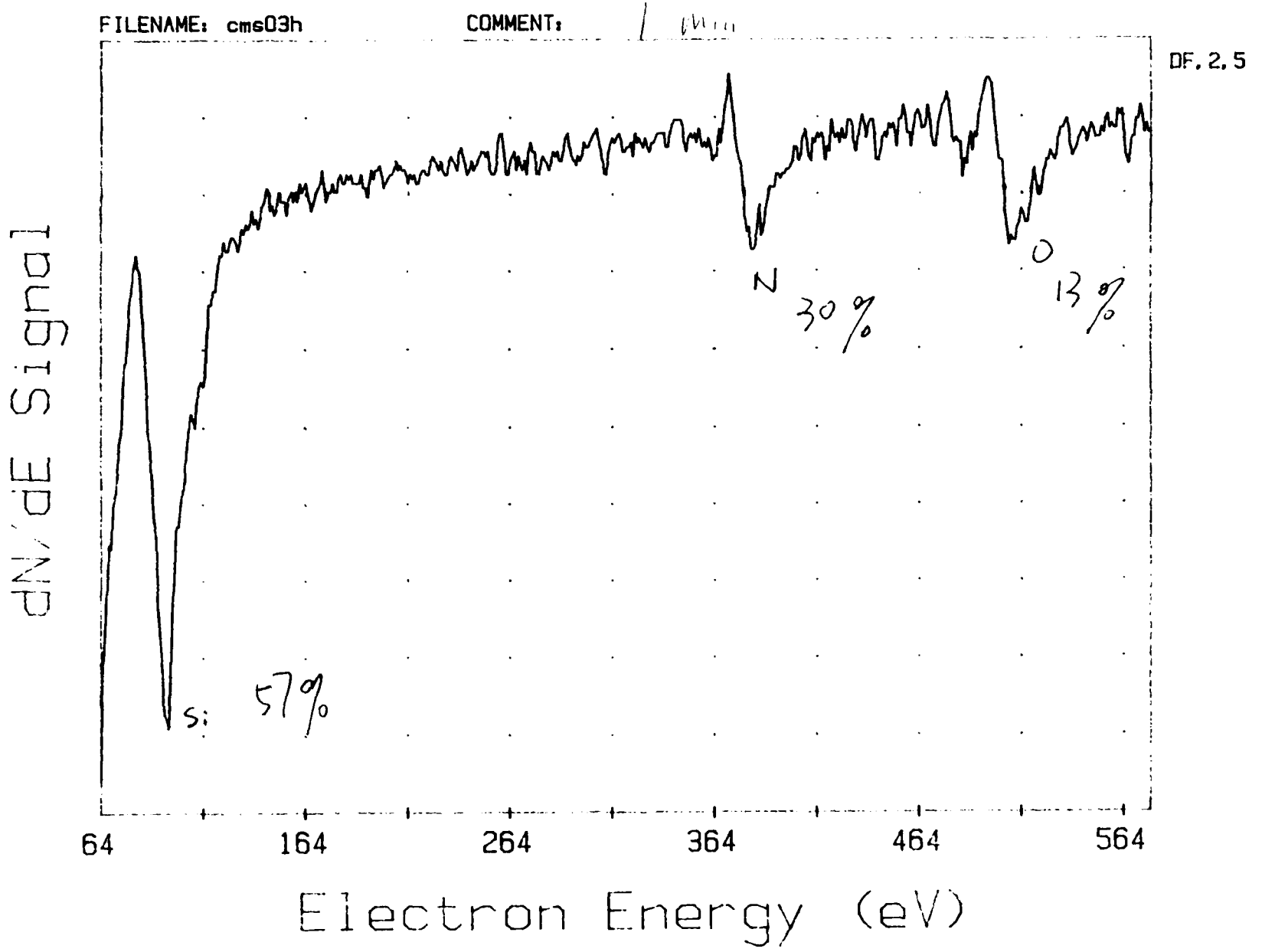
FILENAME: cms03h
COMMENT:
DF, 2, 5
dN/dE Signal
S: 57%
N
30%
O
13%
64
164
264
364
464
564
Electron Energy (eV)

3. Pulsed Laser Deposition of AlN Thin Films

AlN films were grown by laser ablation of AlN powder. The band gap of the smooth films was 6.15 eV. The IR spectrum is characteristic of AlN. The rapid growth rates could exceed 70 nm/min.

Because of its desirable properties many methods have been tried to produce AlN thin films. These include reactive ion-beam sputtering [3.1,2], remote plasma deposition [3.3], rf sputtering [3.4,5], and organometallic chemical vapor deposition[3.6-8] . Among the disadvantages of these methods is that they can cause thermal or plasma damage to the substrate or substrate-film interface. Laser-induced chemical vapor deposition (LI-CVD) avoids this problem and can operate at substrate temperatures between 170°C and 200°C [3.9]. Another promising technique is for growing AlN at low temperatures is reactive molecular-beam epitaxy [3.10].

The method that we used was laser ablation, which has been used to grow many different types of epitaxial films and has had good success with ceramic materials. Ablation from AlN substrate targets had previously been used to grow AlN thin films on sapphire substrates heated to 670 and 500 ^{o}C [3.11]. In the last decade there have been many experimental and theoretical investigations of laser ablation [3.12]. It appears to be the only method that can transfer complex monolayer structures from ceramic targets onto substrates [3.13,14] and is well suited to the growth of AlN films. Heteroatom impurities are not a problem as they are in as CVD, especially where organometallic starting materials are used. Most importantly the ablation growth rate is rapid (73 nm/min).

High purity AlN powder was hydraulically compressed into a tablet. The tablet was placed opposite a quartz window and oriented at 90° to the laser beam. Films were grown on KBr, Suprasil quartz, glass, and GaAs substrates by 248 nm (KrF) or 193 nm (ArF)

excimer laser beams. The laser was softly focussed by a 160 mm focal length lens so that the beam cross-section at the pellet was greater than 4 mm^2. A tightly focussed beam has such a high intensity that it breaks the substrate and ejects small particles.

The growth rates depends on the distance between the ablation point and the substrate. To produce uniform films over 0.5 cm^2 the separation had to be greater than 2 cm. The bes: results were obtained when the substrate was located 3 cm from the focal point. Table 3.1 gives the growth rate as a function of 193 nm laser fluence. The nonlinear increase of growth rate with the laser fluence, implies that the ablation is a multiphoton processes which agrees with other results. It indicates that plasma heating (which would be linear) is not as important as the plasma formation process. At fluences above 4 J/cm^2 a 1 μm film could be grown within 10 minutes compared to rf sputtering (4 - 5 nm/min) [3.4] and remote plasma deposition (4 nm/min) [3.3].

TABLE 3.1

Ablation Film Growth Rates

Laser fluence (J/cm2)	0.3	0.8	2.2
Growth rate (nm/min)	4.0	12.0	72.5

Films were smooth under 1000 X magnification when grown under the best conditions, but "platelets" and non-uniform growth were observed when the pellet was placed close to the focus. Figure 3.1 shows the IR spectrum of a film grown on KBr. The band between 500 and 900 cm^{-1} is due to three phonon modes of AlN: LO at 737 cm^{-1}, TO_1 at 665 cm^{-1} and TO_2 at 630 cm^{-1} [15]. The strong absorption indicates that the composition of the film is mainly AlN. Weak peaks are due to water (3300 cm^{-1} and 1550 cm^{-1}), CO_2 (2350 cm^{-1}) in the spectrometer path and are not from the sample. No other peaks were

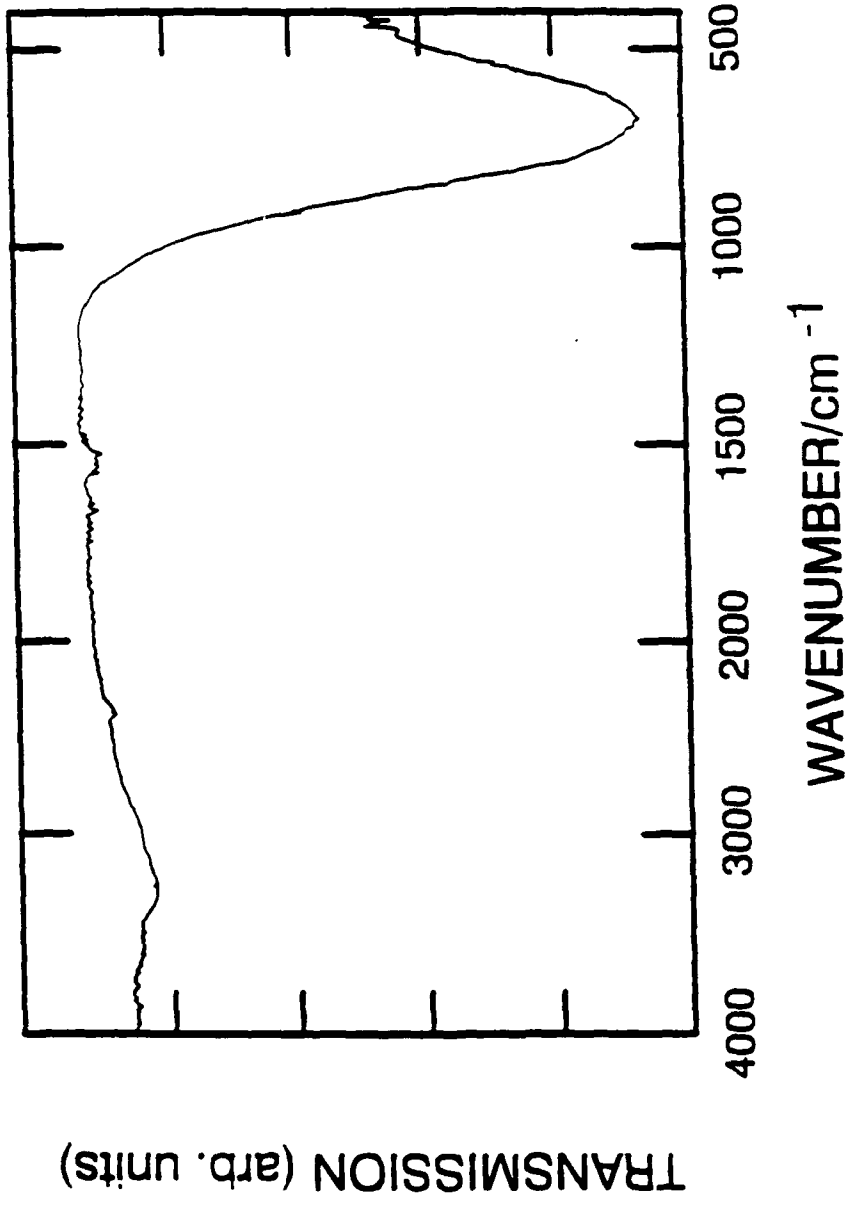

IR transmittance spectrum of a 1 μm AlN film grown on a KBr plate.

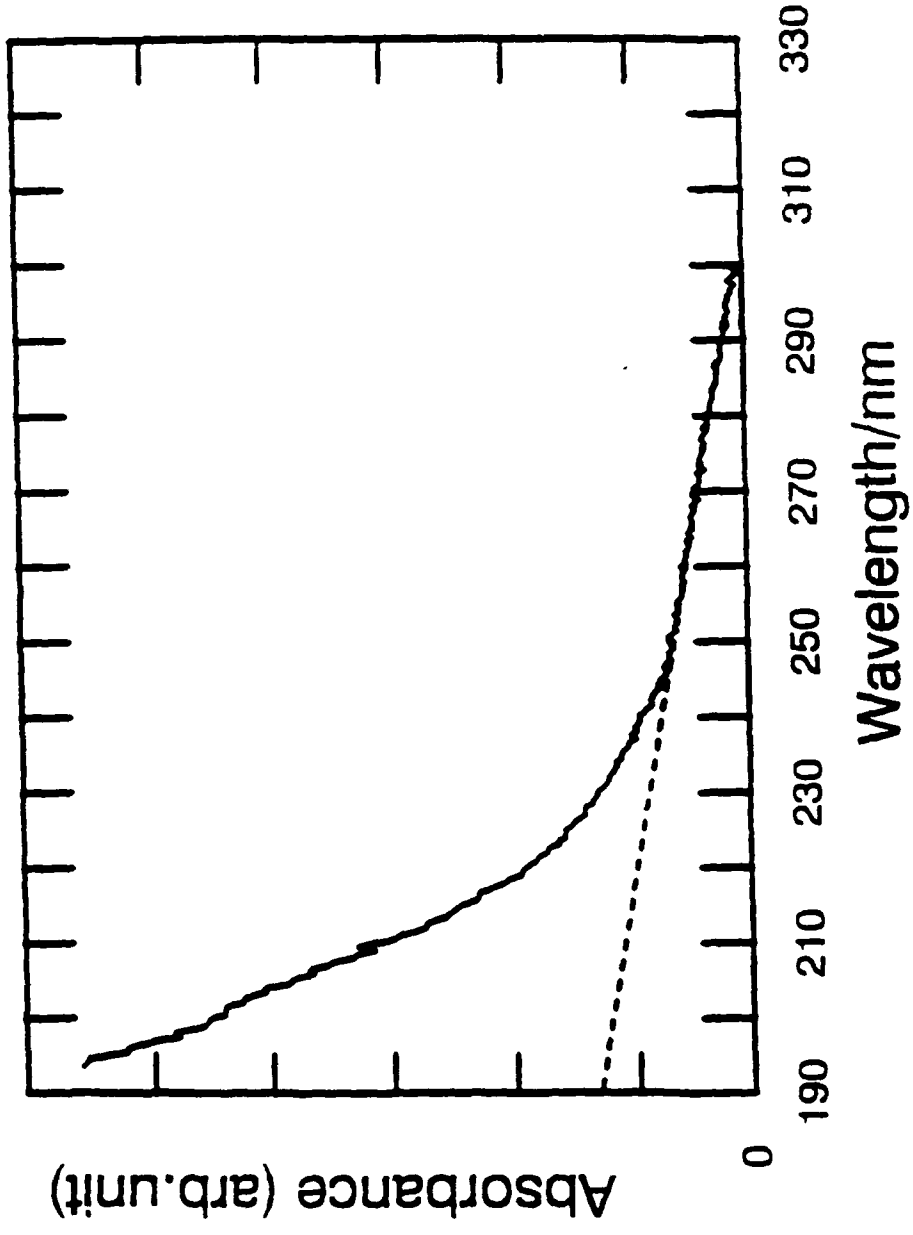

UV absorption spectrum of an AlN film grown on a quartz plate. The broken line estimates scattering from the sample surface.

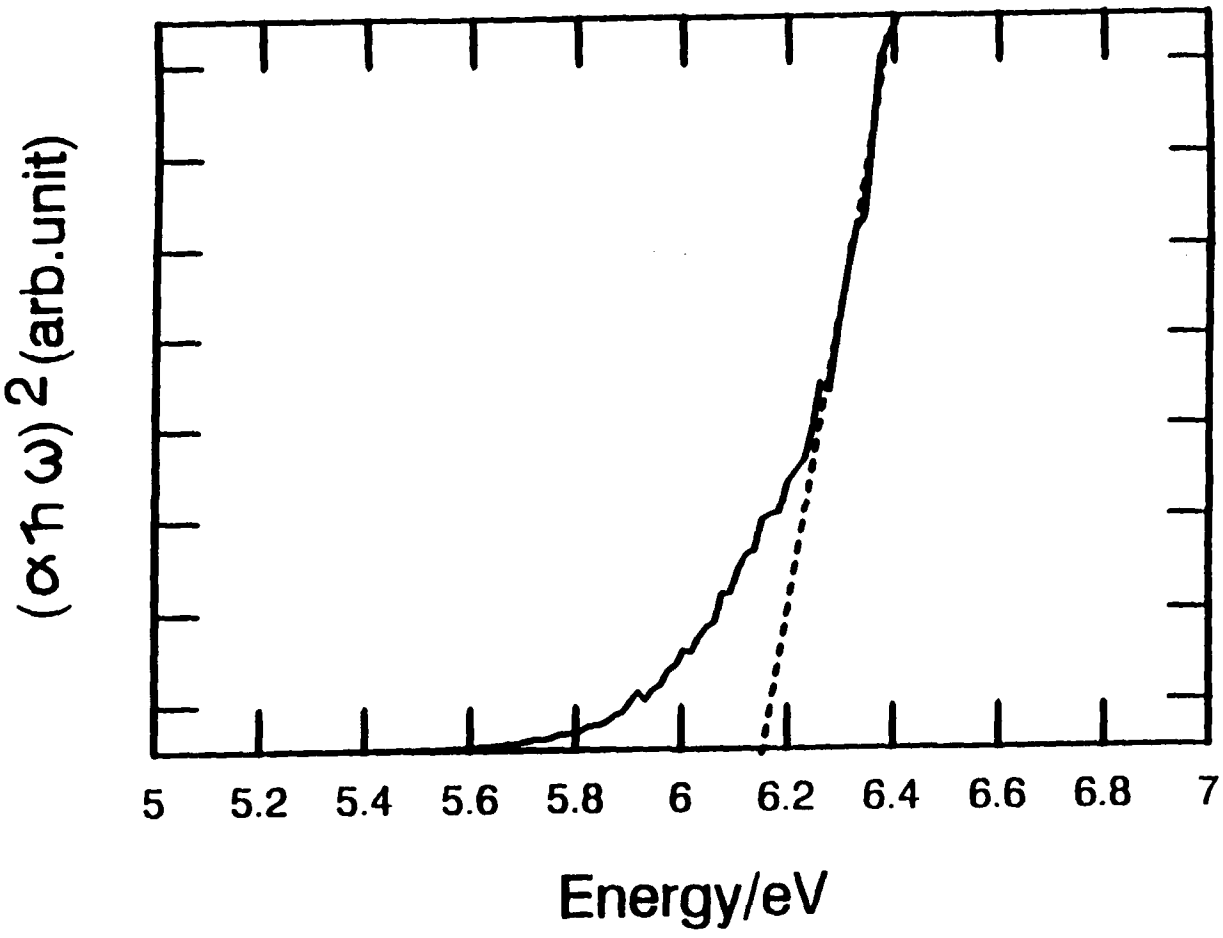

A plot of the square of (absorbance)×(photon energy) as a function of photon energy. This was taken from the UV absorption spectrum of AlN film corrected for surface scattering and reflection. It shows the band gap of 6.15eV for AlN film.

observed. The absence of any Al-O absorption at 460 cm^{-1} is especially important because the oxygen content of the powder was approximately 1% Al_2O_3 [3.17]. Since Al-O bonds are below the detection limit, the deposition rate for AlN must be faster than that for Al_2O_3.

The UV spectrum of an AlN film grown on Suprasil quartz is shown in Figure 3.2. Scattered light is a problem in the UV. A corrected spectrum is plotted in Figure 3.3. The measured AlN band gap E_g is 6.15 eV, which agrees well with that of crystalline AlN (6.2 eV) [3.7,8]. The slow rise above 6 eV is due to either diffuse scattering, sub-bandgap absorptions, or an impurity.

The resistivity of the films was measured for a 1 μm thick film on GaAs substrate. Given the low resistivity of the substrate only a lower limit of 10^9 Ohms/cm for the AlN film could be set, indicating that the film was not conductive aluminum.

An Auger spectrum depth profile was obtained for an AlN film grown by laser ablation. The major constituents were Al and N, with no observable O atom inclusion. Some C atoms were seen on the surface, which were attributed to handling of the sample.

We have demonstrated that the optical properties of AlN films grown by UV laser ablation are equivalent to those of AlN films grown by other methods. Laser ablation growth rates are extremely rapid. The laser ablation method holds excellent promise for the development of AlN films for electronics. In addition to the need for single crystal material for devices, polycrystalline AlN is used for insulating layers, heat sink and for the fabrication of thin film resisters. Laser ablation growth at low temperature is well suited to such applications.

4. Laser Induced CVD Processes Using Trimethyl Aluminum

Trimethylaluminum (TMA) is an important precursor for CVD deposition of aluminum and GaAlAs. Laser induced CVD [1-4] allows growth at lower substrate

temperatures and limits heteroatom interdiffusion [5-7]. Beuermann and Stuke showed that the primary photochemical process is methyl radical detachment [3]. Aluminum atoms are formed from the dimethyl aluminum.

At room temperature, gaseous TMA is a dimer. The monomer only becomes the majority species near 100 ^{o}C [8,9]. Figure 4.1 shows the absorption spectrum at 25 and 125 ^{o}C. The monomer has a strong absorption at short wavelengths and a weak, long wavelength absorption while the dimer does not absorb above 220 nm. Previous LICVD studies of TMA were done at room temperature, therefore, the photochemical reaction must have involved dimers and not monomers. Aluminum deposition from these two species have not been differentiated. While this should make little practical difference for pyrolysis, at least where the molecules striking the surface have been heated so that they are all monomers, the distinction is important for LICVD.

In the dimer two methyl groups are shared between the aluminum atoms forming bridges in a lozenge like structure. Monomer absorption above 210 nm is e' to a_2" or a_2' to a_2" [10]. These types of transitions are weak. There is no equivalent absorption band in the dimer. Both the dimer and the monomer have strong Rydberg bands at 193 nm. Deposition from dimers should always be less efficient because of the necessity of breaking the two additional Al-C bonds.

We grew aluminum films from TMA between 20 °C and 150 °C using KrF (248 nm) and ArF (193 nm) lasers. Auger analysis showed that the films were all esentially pure aluminum, with only minor oxygen and carbon contamination. Figure 4.2 shows the thickness of aluminum films grown by 248 nm LICVD as a function of substrate temperature. The partial pressure of the TMA was 1 torr. The ordinate on the right side of the figure gives the mole fraction of monomer present at various pressures.

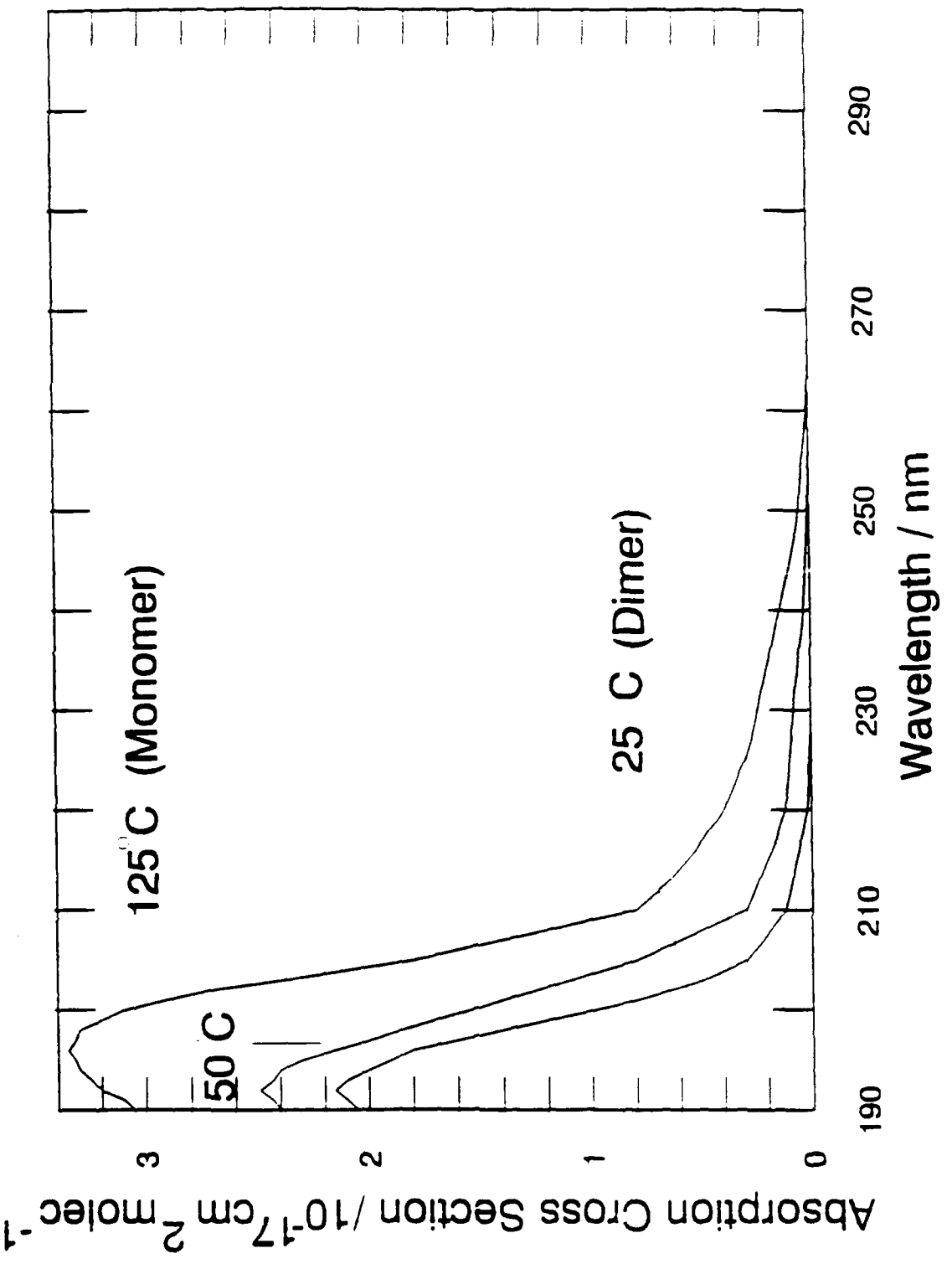
Absorption Cross Section /10-17cm2molec-1
0
1
2
3
190
210
230
250
270
290
Wavelength / nm
125°C (Monomer)
50°C
25°C (Dimer)

The 193 nm laser quickly deposited aluminum on the inside surface of the cell window, attenuating the laser light before it reached the substrate. Even when hydrogen was injected near the window aluminum growth on the substrate by 193 nm light was small and the reproducibility was poor because of light absorption between the window and the substrate.

TABLE 4.1

Relative Quantum Yields of Al Films Grown by LICVD

Wavelength (nm)	State	Temperature (^{o}C)	Depostion Rate (nm/min)	σ 10^{-18} molec-cm^2	Relative Quantum Yield
193	Monomer	120 ± 2	1200	31.0	1.00
	Dimer	25 ± 2	260	20.0	0.34
248	Monomer	120 ± 2	110	0.8	3.50
	Dimer	25 ± 2	—	0.1	<0.50

To compare growth of the monomer and dimer at 193 and 248 nm films were grown on the inside surface of the vacuum cell window which could be heated. The results are summarized in Table 4.1. Yields were normalized to the number of absorbed photons. The relative quantum yield refers to the film thickness for an equivalent number of laser shots at 5 mJ/cm^2-pulse and 10 Hz. The yield for 193 monomer is arbitrarily taken as the reference. Al deposited on the window attenuates the light and the deposition rate depends on the amount of aluminum that was previously deposited. To control for this the film in all runs was grown to about 0.3 μm. This would lead to an underestimate the efficiency under the most efficient growth conditions. Growth from dimers is less efficient at 193 and 248 nm.

At 248 nm, the film grown from dimers was too thin to measure with the profilemeter. Growth from the monomer at 248 is 3.5 times as efficient as that at 193 nm.

The fraction of monomer depends on the temperature and the partial pressure of TMA in the cell. The TMA partial pressure was about 1 Torr. Only the TMA near the substrate was warmed by the heater, thus only the molecules near the substrate were monomers. Figures 4.2 shows that 248 nm deposition correlates with the mole fraction of monomer near the substrate. Accounting for the mole fractions of monomers and dimers at 20°C and 150°C and the absorption coefficient of both species at 248 nm, one would expect an 8 to 1 ratio in the efficiency of aluminum film growth. The actual ratio is at least 15 to 1, where the growth from dimers is an upper limit. Thus, even on a per molecule of TMA, per photon absorbed basis deposition from the monomer is at least twice as efficient as that from the dimer. The experiments summarized in Table 4.2 decrease the lower limit to this efficiency ratio to 7:1 on the same basis.

Beuermann and Stuke [3] suggested the following mechanisms for monomer photolysis in the UV region (190 - 300 nm):

$$Al(CH_3)_3 + hv \text{ ----> } Al(CH_3)_2^* + CH_3 \qquad (A),$$

$$Al(CH_3)_2^* \text{ ----> } Al + C_2H_6 \qquad (B),$$

$$Al(CH_3)_3 + hv \text{ ----> } AlCH_3 + 2CH_3 \qquad (C),$$

where $Al(CH_3)_2^*$ is metastable. Process (C) dominates below 210 nm and process (A) followed by process (B) dominates above 230 nm. Aluminum atoms are produced by single photon photolysis of monomers at 248 nm . Motooka et al. [4.1] showed that the first step in dimer photolysis is separation into monomers. Therefore, dimer photolysis cannot be as effective as monomer photolysis, because it requires absorption of an additional photon to produce an aluminum atom.

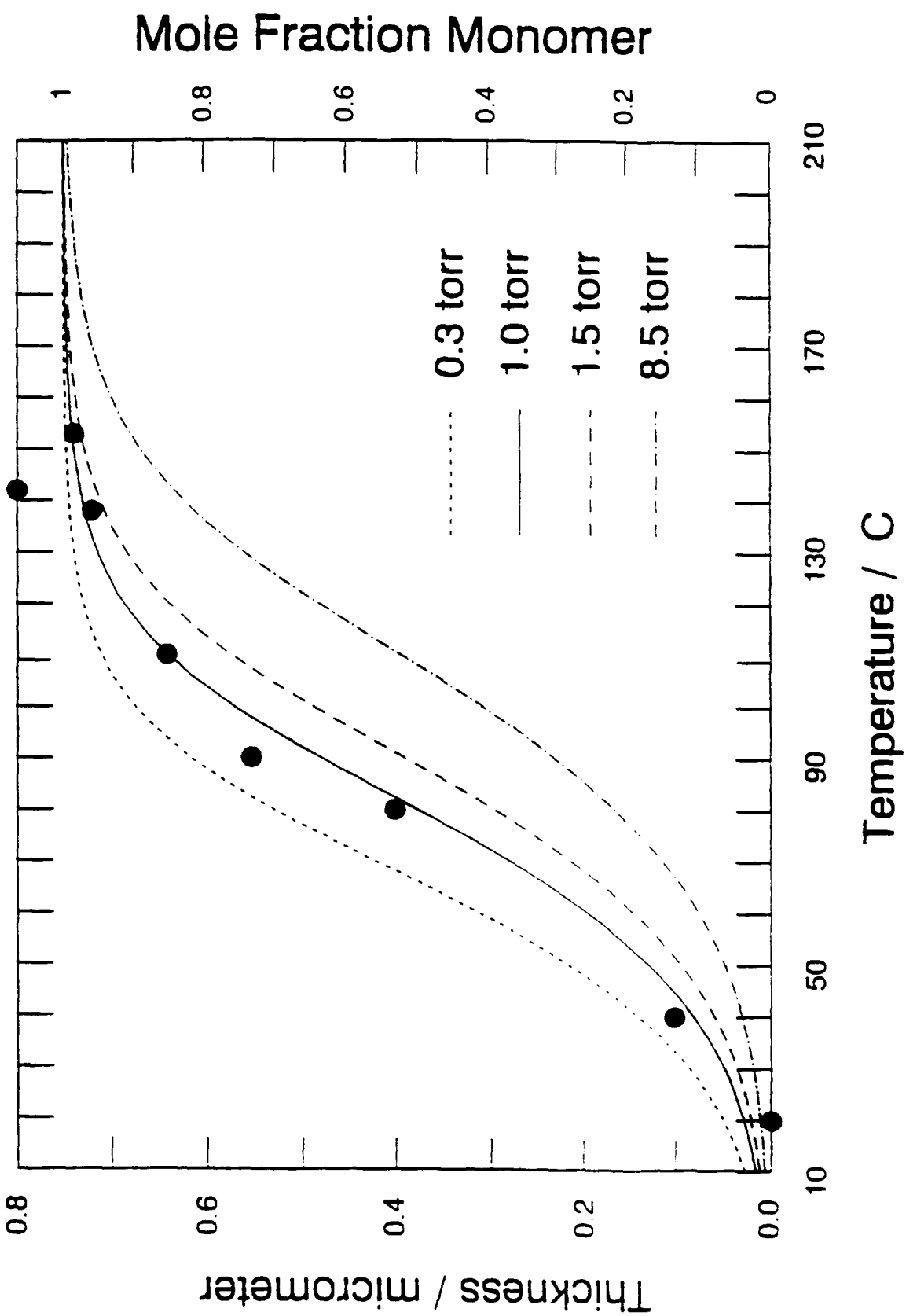
Mole Fraction Monomer
1
0.8
0.6
0.4
0.2
0
0.3 torr
1.0 torr
1.5 torr
8.5 torr
210
170
130
90
50
10
Temperature / C
Thickness / micrometer
0.8
0.6
0.4
0.2
0.0

Laser heating of the substrate is unimportant. The quartz substrate is transparent at 193 and 248 nm. The aluminum films should reflect the laser light. Little energy should be deposited into the substrate or film to produce heating and no heating was measured Moreover, if laser heating were important similar results should be seen at 193 and 248 nm. The temperature dependence shows that surface reactions are not controlling. The coverage of physisorbed TMA decreases with increasing temperature. If surface reactions were rate limiting the deposition rate would do the same. Surface reactions may play a role, but the controlling process is the homogeneous gas phase photolysis.

In light activated CVD processes typically, much of the incident light does not reach the region near the substrate but is absorbed by molecules lying between the substrate and the window. In the method discussed here, the substrate was heated to 130°C and illuminated with 248 nm light. Because TMA is almost completely dimerized except near the substrate, the 248 nm light was not absorbed in the middle of the cell and there was no coating of the entrance window. Only the monomeric TMA near the heated substrate absorbed 248 nm light and aluminum atoms were produced only near the substrate, where they effectively formed a film. Furthermore, the yield of aluminum per 248 nm photon absorbed by the monomer is substantially higher than that from the dimer and higher than that formed from the monomer at 193 nm. Thus 248 nm photolysis of TMA near a warm substrate is a superior LICVD method for aluminum film growth at relatively low temperatures (100 °C < T <150 °C).

5.0 References

2.1. S.L. Ahang, J.T. Wang, W. Kaplan and M. Ostling, Thin Solid Films, **213** (1992) 182.

2.2. C.H. Ling, C.Y. Kwok and K. Prasad, J. Vac. Sci. Technol. A., **5** (1987) 1874.

2.3. T. Ito, S. Hijiya, T. Nozaki, H. Arakawa, M. Shinoda and Y. Fukukawa, J. Electrochem. Soc., **125** (1978) 448.

2.4. S. Yokoyama, N. Kajihara, M. Hirose, Y. Osaka, T. Yoshihara and H. Abe, J. Appl. Phys., **51** (1980) 5470.

2.5. J.C. Barbour, H.J.Stein, O.A.Popov, M. Yoder and C.A. Outten, J. Vac. Sci. Technol. A, **9** (1991) 480.

2.6. V.I. Belyi, et al., SiliconNitride in Electronics (Elsevier Science Publishers, 1988) p 154.

2.7. A. Iqbal, W.B. Jackson, C.C. Tsai, J.W. Allen and C.W. Bates, Jr., J. Appl. Phys., 61 (1987) 2947.

2.8. J.T. Cheung and H. Sankus, CRC Critical Reviews in Solid State and Materials Sciences 15 (1988) 63.

3.1. U. Mazur and A.C. Cleary, J. Phys. Chem. **94**, (1990)189.

3.2. E.I. Meletis and S. Yan, J. Vac. Sci. Technol. **A9**, (1991) 2279

3.3. H. Nomura, S. Meikle, Y. Nakanishi, and Y. Hatanaka, J. Appl. Phys., **69**, (1991) 990.

3.4. W. Dehuang, G. Liang, Z. Suzhen, Z. Xia, and Y. Jinzhong, Thin Solid Film, **187**, (1990)127.

3.5. K. Kubota, Y. Kobayashi, and K. Fujimoto, J. Appl. Phys., **66**, (1989) 2984.

3.6. M. Morita, S. Isogai, N. Shimizu, K. Tsubouchi, N. Mikoshiba, Jpn. J. Appl. Phys., **20**, (1981) L173.

3.7. M. Morita, K. Tsubouchi, and N. Mikoshiba, Jpn. J. Appl. Phys., **21**, (1982)102.

3.8. W.M. Yim, E.J. Stofko, P.J. Zanzucchi, J.I. Pankove, M. Ettenberg, and S.L. Gilbert, J. Appl. Phys., **44**, (1973).292.

3.9. X. Li and T.L. Tansley, J. Appl. Phys., **68**, (1990) 5369.

3.10. H.-U. Baier and W. Mönch, J. Appl. Phys., **68**, (1990) 586.

3.11. M.G. Norton, P.G. Kotula and C.B. Carter, J. Appl. Phys.**70**, (1991) 2871.

3.12. B. Fain and S.H. Lin (and references therein), J. Chem. Phys., **91**, (1989) 2726.

3.13. R.B. Laibowitz, R.H. Kock, P. Chaudharri, and R.J.Gambino, Phys. Rev., **B35**, (1987) 8821.

3.14. A. Cohen, P. Allenspacher, M.M. Brieger, I. Jeuck, and H. Opower, Appl. Phys. Lett., **59**, (1991) 2186.

3.15. A.T. Collins, E.C. Lighthouse, and P.J. Dean, Phys. Rev. **158**, (1967)833.

3.16. H. Demiryont, L.R. Thompson, and G.L. Collins, J. Appl. Phys. **59**, (1986) 3235.

3.17. N. Kuramoto, H. Taniguchi, and I. Aso, Proc. 36th Electron Compon. Conf., (Institute of Electrical and Electronic Engineers, Inc., New York, 1984)p. 424.

3.18. J.I. Pankove, Optical Processes in Semiconductors (Dover, New York, 1975).

4.1. T.Motooka, S.Gorbatkin, D.Lubben, and J.E.Greene, J. Appl. Phys., **58** (1985) 4394 .

4.2. G.S.Higashi, J.Chem.Phys., **88** (1988) 422 .

4.3. Th. Beuermann and M. Stuke, Chem. Phys. Lett., **178** (1991) 197.

4.4. S.A. Mitchell and P.A. Hackett, J. Chem. Phys., **79** (1983) 4815, Chem. Phys. Lett., **107** (1984) 508.

4.5. D.J. Ehrlich, R.H. Osgood,Jr., and T.F. Deutsch, IEEE J. Quantum Electro., **6** (1980) 1233 .

4.6. D.J. Ehrlich and J.Y. Tsao, J. Vac. Sci. Technol., **B1**, (1983) 969.

4.7. R.M. Osgood and T.F. Deutsch, Science **227** (1985) 709.

4.8. A.M. Laubeugayer and W.F. Gillian, J. Am. Chem. Soc., **63** (1941) 477.

4.9. M.B. Smith, J. Or ganometal. Chem,. **46** (1972) 31.

4.10. H. Okabe, M.K. Emadi-Babaki and V.R. McCrary, J. Appl. Phys., **69** (1991) 1730.

4.11. A. Amirav, A. Penner and R. Bersohn, J. Chem. Phys., **90** (1989) 5232.

6.0 Written Publications

"Laser induced chemical vapor deposition of aluminum from trimethylaluminum: wavelength and temperature dependence", K. Seki, J.M. Frye, H. Okabe and J.B. Halpern. To be published in the Journal of Crystal Growth (in proof).

"Room temperature growth of AlN thin films by laser ablation", K. Seki, X. Xu, H. Okabe, J.M. Frye and J.B. Halpern. Applied Physics Letters, 60 (1992) 2234.

"Pulsed laser desorption of thin silicon nitride films", X. Xu, K. Seki, N. Chen, H. Okabe and J.B. Halpern. Materials Research Society Proceedings, 285 (1993) 331.

7.0 Professional Personnel

Dr. Joshua B. Halpern	Ph.D. (Physics), June 1972, Brown University
Dr. Joan M. Frye	Ph.D. (Chemistry), June 1985, University of Chicago
Dr. Hideo Okabe	Ph.D. (Chemistry), June 1955, University of Rochester
Dr. Kanekazu Seki	Ph.D. (Chemistry), June 1986, University of Tokyo

8.0 New Discoveries and Inventions

1. Photoablative growth of AlN films from AlN powders at low temperature.
2. Photoablative growth of SiN films from SiN powders at low temperature.
3. New process for laser induced chemical vapor deposition of Al or aluminum containing films from trimetylaluminum.

Room-temperature growth of AlN thin films by laser ablation

Kanekazu Seki, Xiangqun Xu, Hideo Okabe, Joan M. Frye, and Joshua B. Halpern
Department of Chemistry and Materials Science Research Center of Excellence, Howard University, Washington, D.C. 20059

(Received 13 November 1991; accepted for publication 26 February 1992)

Excimer laser ablation of compressed AlN powder has been used to grow thin AlN films at room temperature on a variety of substrates. The films have a band gap of 6.15 eV as measured by UV absorption. Examination with a scanning electron microscope and an optical microscope shows that the films are smooth. The IR spectrum has an absorption characteristic of AlN. Growth rates are extremely rapid, exceeding 70 nm/min.

Because of desirable electrical, optical, dielectric, thermal, and acoustical properties many methods have been tried to produce AlN thin films. These include reactive ion-beam sputtering,[1,2] remote plasma deposition,[3] rf sputtering,[4,5] and organometallic chemical vapor deposition.[6-8] Each of these methods has disadvantages. For example, most of them can cause thermal or plasma damage to the substrate or substrate-film interface. A new method designed to avoid thermal degradation, laser-induced chemical vapor deposition (LICVD), has been demonstrated at substrate temperatures between 170 and 200 °C.[9] Another promising technique is reactive molecular-beam epitaxy for growing AlN films at room temperature.[10]

This letter reports growth of AlN thin films at room temperature from AlN powder tablets using laser ablation, a method that has been used to grow many different types of epitaxial films. Ablation from AlN substrates had previously been used to grow AlN thin films on sapphire substrates heated to 670 and 500 °C.[11]

Laser ablation is particularly well suited to growth of refractory material films. In the last decade there have been many experimental and theoretical investigations of laser ablation,[12] especially for production of high-temperature superconducting films. It appears to be the only method that can transfer complex monolayer structures from ceramic targets onto substrates.[13,14] Ablation thus appears to be well suited to the growth of AlN films.

AlN films grown by laser ablation should not contain heteroatom impurities as would films grown by CVD, which are often degraded by carbon and other impurities originating in organometallic starting materials. Furthermore, the ablation growth rate has proved to be rapid (73 nm/min).

In this work, AlN powder (Strem Chemicals Inc. 98% purity) was compressed in a die used to prepare samples for IR analysis. The die was placed in a hydraulic press (2.5 ton/cm^2) and a small tablet, 13 mm in diameter and 2 mm in thickness, was formed.

Figure 1 is a diagram of the inside of the stainless steel vacuum chamber used for growth. The tablet was placed opposite a quartz window and oriented at 90° to the laser beam. The substrate can be placed in any position around the powder tablet. Films were grown on KBr, Suprasil quartz, glass, and GaAs substrates. Irradiation at 248 nm (KrF) or 193 nm (ArF) was provided by a pulsed, 20 ns pulse width, 10 Hz excimer laser. The laser was softly focused by a 160-mm-focal length lens. The laser fluence at the powder pellet was between 0.2 and 4.0 J/cm^2 pulse. The beam cross section at the pellet had a diameter greater than 2 mm because the intensity of a tightly focused beam is so high that it can break the sample pellet and eject small particles. The cell was evacuated by a two-stage mechanical pump which produced a background pressure of 10^{-3} Torr. All experiments were carried out at room temperature.

Growth rates strongly depended on the distance between the laser focal point and the substrate. To grow uniform films over a 0.5 cm^2 area the distance had to be at least 2 cm. Typically, best results are obtained when the substrate was located 3 cm from the focal point. To avoid contamination with powder ejected by the ablation, the substrate was usually placed to the side of the tablet, although it could also be placed above it. The growth rate as a function of laser fluence at 193 nm is given in Table I. Film thickness was measured by a depth profilometer.

The growth rate increases nonlinearly with a laser fluence, indicating that ablation is a multiphoton processes. A 1 μm film could be grown within 10 min at fluences above 4 J/cm^2. This is extremely rapid compared to rf sputtering method (4–5 nm/min)[4] and remote plasma deposition (4 nm/min).[3] Since 400 Hz excimer lasers are available with comparable fluences, a forty-fold increase in growth rate is possible. Rapid growth is one remarkable advantage of the laser ablation method for AlN film growth.

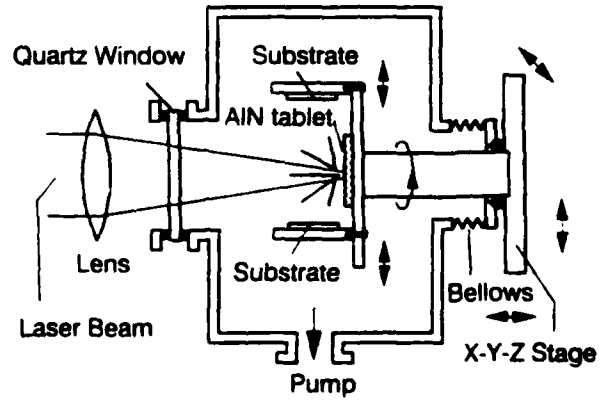

FIG. 1. Inside of vacuum chamber for ablation film growth. Substrates can be mounted in any position around the ablation beam. The laser fluence ranged between 0.2 and 4 J/cm^2 per pulse in a cross section of about 2 mm diam at the target.

 0003-6951/92/182234-03$03.00

TABLE I. Ablation film growth rates.

Laser fluence (J/cm^2)	0.3	0.8	2.2
Growth rate (nm/min)	4.0	12.0	72.5

The films were examined at magnifications up to 1000 by a scanning electron microscope and an optical microscope. Films were smooth when grown under the best conditions, but "platelets" and nonuniform growth were observed when the pellet placed close to the laser focus.

Figure 2 shows the IR transmittance spectrum of an AlN film grown on KBr taken using a Perkin–Elmer Model 1600 FTIR spectrometer. The broad band between 500 and 900 cm^{-1} is due to the phonon modes of AlN: LO at 737 cm^{-1}, TO_1 at 665 cm^{-1} and TO_2 at 630 cm^{-1}.[15] The strong phonon mode indicates that the composition of the film is mainly AlN.

Other weak peaks seen in this spectrum can be assigned to water (3300 and 1550 cm^{-1}), CO_2 (2350 cm^{-1}), and air in the spectrometer path and are not from the sample. No other peaks were observed. Especially significant is the absence of absorption from any Al—O bond at 460 cm^{-1}.[16] The oxygen content of AlN powders is approximately 1% as Al_2O_3.[17] Since Al_2O_3 inclusions are below the detection limit, less than 1% of AlN, the laser ablation deposition rate for AlN must be faster than that for Al_2O_3.

The UV spectrum of AlN films grown on a Suprasil quartz plate was measured by a Cary 2390 (Varian) spectrophotometer and is shown in Fig. 3. The optical absorption coefficient, α depends on the photon energy $\hbar\omega$ and the band-gap E_g:[18]

$$\alpha = [\hbar\omega - E_g]^{1/2}/\hbar\omega. \quad (1)$$

Thus, E_g can be obtained from the UV spectrum using Eq. (1). However, surface light scattering is very large in the UV and the real absorption spectrum is difficult to obtain: reflection losses should also be considered.[8] In order to estimate the band gap of the AlN film and/or additional subband gaps, the broken line in Fig. 3 was taken as the scattering baseline. The corrected spectrum is plotted in

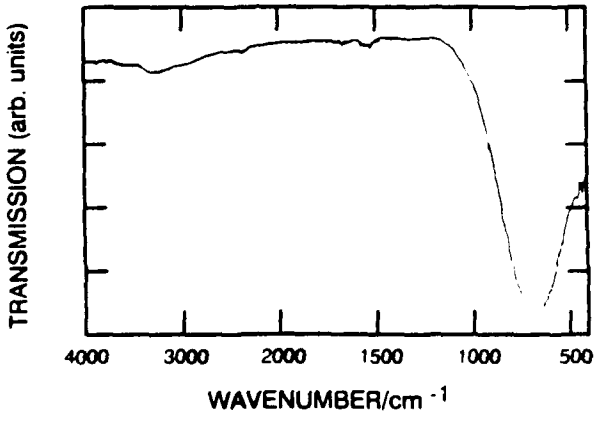

FIG. 2. IR transmittance spectrum of a 1 μm thick AlN film grown on a KBr plate.

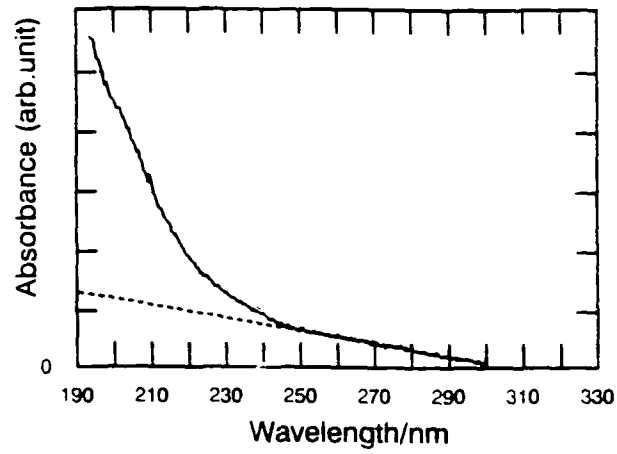

FIG. 3. UV absorption spectrum of an AlN film grown on a quartz plate. The broken line estimates scattering from the sample surface.

Fig. 4, where it can be seen that $(\hbar\omega\,\alpha)^2$ depends linearly on $\hbar\omega$ in the high energy region. Linear regression analysis yields an AlN band gap E_g of 6.15 eV, which agrees well with that of crystalline AlN (6.2 eV).[7,8] The slow rise in the low energy region above 6 eV is due to either remnant diffuse scattering, additional subband-gap absorptions, and/or an impurity.

The resistivity of the deposited material was measured for a 1 μm thick film on a GaAs substrate. Because of the relatively low resistivity of the substrate it was only possible to obtain a lower limit of 10^9 Ω/cm for the AlN film. This cannot be due to Al, it is too high, or to Al_2O_3, because none is seen in the IR spectrum, thus one concludes that the resistivity is consistent with the deposition of AlN.

An Auger spectrum depth profile was obtained for an AlN film grown by laser ablation. The major constituents were Al and N, with no observable O atom inclusion. Some C atoms were seen on the surface, which were attributed to handling of the sample.

It has been demonstrated that the optical properties of

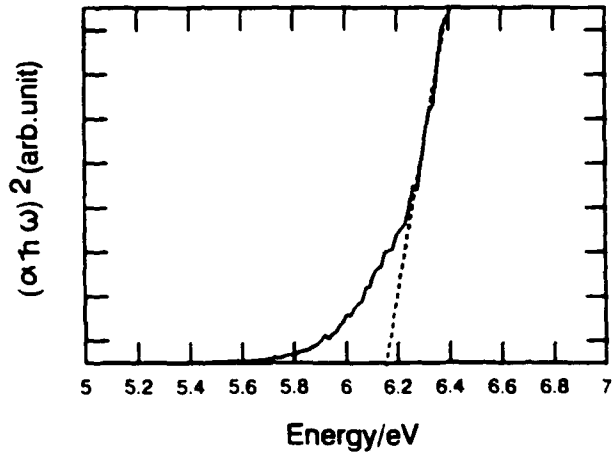

FIG. 4. A plot of the square of (absorbance) × (photon energy) as a function of photon energy. This was taken from the UV absorption spectrum corrected for surface scattering and reflection.

AlN films grown by UV laser ablation are equivalent to those of AlN films grown by other methods. Laser ablation growth rates are extremely rapid. The laser ablation method holds excellent promise for the development of AlN films for electronics. In addition to the need for single-crystal material for devices, polycrystalline AlN is used for insulating layers, heat sink, and for the fabrication of thin-films resistors. Laser ablation growth at low temperatures is well suited to such applications. Work is underway to analyze the AlN film structure by x-ray diffraction.

This work was supported by the U.S. Air Force Office of Scientific Research Contract FQ8671-89-01458 2306/B1.

[1] U. Mazur and A. C. Cleary, J. Phys. Chem. **94**, 189 (1990).
[2] E. I. Meletis and S. Yan, J. Vac. Sci. Technol. A **9**, 2279 (1991).
[3] H. Nomura, S. Meikle, Y. Nakanishi, and Y. Hatanaka, J. Appl. Phys. **69**, 990 (1991).
[4] W. Dehuang, G. Liang, Z. Suzhen, Z. Xia, and Y. Jinzhong, Thin Solid Film **187**, 127 (1990).
[5] K. Kubota, Y. Kobayashi, and K. Fujimoto, J. Appl. Phys. **66**, 2984 (1989).
[6] M. Morita, S. Isogai, N. Shimizu, K. Tsubouchi, and N. Mikoshiba, Jpn. J. Appl. Phys. **20**, L173 (1981).
[7] M. Morita, K. Tsubouchi, and N. Mikoshiba, Jpn. J. Appl. Phys. **21**, 1102 (1982).
[8] W. M. Yim, E. J. Stofko, P. J. Zanzucchi, J. I. Pankove, M. Ettenberg, and S. L. Gilbert, J. Appl. Phys. **44**, 292 (1973).
[9] X. Li and T. L. Tansley, J. Appl. Phys. **68**, 5369 (1990).
[10] H.-U. Baier and W. Mönch, J. Appl. Phys. **68**, 586 (1990).
[11] M. G. Norton, P. G. Kotula, and C. B. Carter, J. Appl. Phys. **70**, 2871 (1991).
[12] B. Fain and S. H. Lin (and references therein), J. Chem. Phys. **91**, 2726 (1989).
[13] R. B. Laibowitz, R. H. Kock, P. Chaudharn, and R. J. Gambino, Phys. Rev. B **35**, 8821 (1987).
[14] A. Cohen, P. Allenspacher, M. M. Brieger, I. Jeuck, and H. Opower, Appl. Phys. Lett. **59**, 2186 (1991).
[15] A. T. Collins, E. C. Lighthouse, and P. J. Dean, Phys. Rev. **158**, 833 (1967).
[16] H. Demiryont, L. R. Thompson, and G. L. Collins, J. Appl. Phys. **59**, 3235 (1986).
[17] N. Kuramoto, H. Taniguchi, and I. Aso, *Proceedings of the 36th Electron Component Conference* (Institute of Electrical and Electronic Engineers, New York, 1984), p. 424.
[18] J. I. Pankove, *Optical Processes in Semiconductors* (Dover, New York, 1975).

PULSED LASER DEPOSITION OF THIN SILICON NITRIDE FILMS

XIANGQUN XU, KANEKAZU SEKI, NAIQUN CHEN, HIDEO OKABE, JOAN M. FRYE AND JOSHUA B. HALPERN Materials Science Research Center of Excellence and Department of Chemistry, Howard University, Washington, DC 20059

Pulsed laser deposition of compressed Si_3N_4 powder has been used to grow thin SiN_x films on a variety of substrates at substrate temperatures ranging from room temperature to 350 °C. Film composition was analyzed by Auger electron spectroscopy. The $SiN_{0.33}$ films have a band gap of 5.60 eV as measured by UV absorption. The FT-IR spectrum shows an absorption characteristic of Si-N. The Si/N ratio in the deposited films corresponding to various substrate temperatures has also been determined.

INTRODUCTION

Thin films of high quality silicon nitride are important as dielectric materials and functional memory layers in microelectronic and optoelectronic device.[1-5] Conventional deposition techniques of silicon nitride films include chemical vapor deposition(CVD),[1] plasma enhanced CVD(PECVD),[2] and direct thermal nitridation.[3] Each of these techniques has disadvantages. For example, CVD is a high temperature technique (≥600 °C) which may cause atom migration and/or dopant diffusion in some semiconductors. PECVD uses low deposition temperature (~300 °C) but often incorporate too much hydrogen in the dielectric and may cause damage due to the high energy ions (hundreds to thousands of eV)[5].

Pulsed laser deposition (PLD) has emerged as a powerful means for the deposition of superconducting thin films as well as semiconducting, insulating, ferroelectric and other thin films. This work reports growth of SiN_x films from room temperature to 350°C using pulsed laser deposition. Auger analysis, fourier transform infrared (FT-IR) analysis and UV absorption were used to analyze the composition and properties of the deposited films.

EXPERIMENTAL

Target pellets were prepared by compressing Si_3N_4 powder (electronic grade, Johnson Matthey Co.) in a die similar to that used for IR sample preparation. The die was placed in a hydraulic press (2.5 *ton/cm*^{2}) and a small tablet, 13mm in diameter and 3mm in thickness, was formed. Fig.1 is a diagram of the stainless steel vacuum chamber used for growth. The

Mat. Res. Soc. Symp. Proc. Vol. 285. © 1993 Materials Research Society

target pellet was placed parallel to the substrate and oriented at 45° to the laser beam. This produced a plume of ablated material perpendicular to the target surface and the substrate which was placed at a distance of 3cm from the target. Films were grown on Si (100) wafers, KBr plates and Suprasil quartz plates. Si (100) wafers were cleaned with pure methanol, then dipped in 6% hydrofluoric acid for 30s, rinsed with deionized water and dried in flowing air. Suprasil quartz plates were cleaned with pure acetone. Irradiation at 248 nm (KrF) or 193 nm (ArF) was provided by a pulsed (20 ns width) excimer laser using a repetition rate of 1-10 Hz. The laser was focused by a 160-mm-focal-length lens. The laser fluence at the target pellet was between 1.0-6.0 J/cm^2 per pulse. The substrate temperature was measured by a thermocouple which was directly put on the substrate. After loading the substrate and the target into the vacuum chamber, the chamber was evacuated to 5×10^{-5} torr.

The films were examined by a PHI 590 Scanning Auger, a Perkin-Elmer 1600 FT-IR and a Milton Roy 1201 UV spectrometers. The deposited films were also examined by an Olympus B071 optical microscope. The film thickness was measured by a depth profilometer.

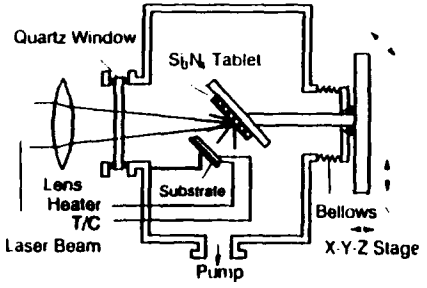

FIG.1. The vacuum chamber for ablation film growth. Substrates were put on a resistance heater. A thermocouple was used to measure the temperature of the substrate surface. The laser fluence ranged from 1.0 to 6.0 J/cm^2 per pulse in a cross section of about 2 mm diameter on the target surface.

RESULTS AND DISCUSSION

The chemical composition of films formed by PLD was examined by Auger electron microscopy (AES). Auger analysis showed the major constituents were Si and N, with the presence of some oxygen and carbon at the surface which was attributed to the residual gas in the chamber and/or to handling of the samples. Fig.2 is an Auger depth profile of a PLD silicon nitride film grown on Si wafer at a substrate temperature of 320 °C in vacuum. This reveals a non-stoichiometric composition with N/Si ratio of about 0.3. The non stoichiometric

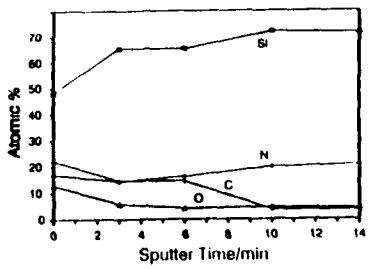

FIG.2. Auger depth profile for a PLD SiN_0, film grown on Si substrate at 320 °C in vacuum.

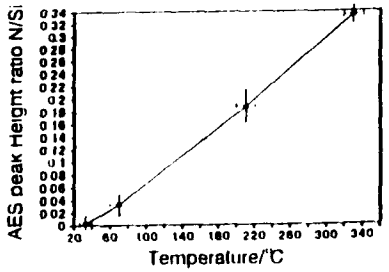

FIG.3. Auger peak height ratio corresponding to various substrate temperatures.

ratio may be due to the presence of strong plasma during the deposition.[6] The ions, molecules and excited neutral atoms produced by the plasma may not recombine evenly on the substrate. Some nitrogen atoms/ions may combine with others to produce nitrogen molecules which remain in the gas phase and are pumped out of the chamber. The films grown in this work were all non-stoichiometric with a N/Si ratio in the range of 0.1-0.4. It was found that the substrate temperature greatly affects the SiN_x film composition. Fig.3 shows Auger peak height ratios at various substrate temperatures. In the Si-rich silicon nitride films, the dominant defects are silicon dangling bonds which can trap either electrons or holes. They may be well suited to TFTs (thin-film transistors) devices since these devices function using electron channels.[7]

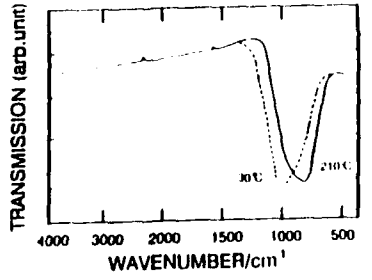

FIG.4. IR transmittance spectrum for silicon nitride films grown at substrate temperatures of 210 °C (solid) and 30 °C (dashed).

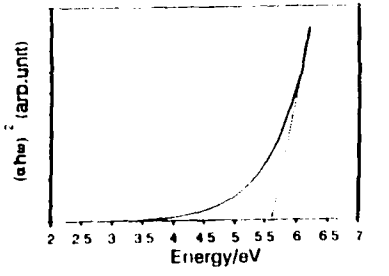

FIG.5. A plot of the square of (absorbance)×(photon energy) as a function of photon energy. This was taken from the UV absorption spectrum of $SiN_{0.3}$ film corrected for surface scattering and reflection. It shows a band gap of 5.60 eV for $SiN_{0.3}$ film.

Fig.4 shows the FT IR transmittance spectrum for silicon nitride films grown at substrate temperatures of 210 °C (solid) and 30 °C (dashed). The film grown at 210 °C has a large absorption peak in the region where one finds the absorption characteristic of Si-N stretching mode (830 - 850 cm^{-1}[8,9]). The absorption peak of the film grown at 30 °C was in the region of SiO_2 antisymmetric stretching mode (~1080 cm^{-1}). Thus films grown at lower temperature contain more oxygen; this suggests a technique for monitoring the oxygen content of PLD films.

The UV absorption spectrum of silicon nitride films grown on a Suprasil quartz was obtained. Since the optical absorption coefficient is given by

$$\alpha = (\hbar\omega - E_g)^{1/2}/\hbar\omega \qquad (1)$$

where $\hbar\omega$ is the photon energy and E_g is the band-gap, E_g can be obtained by linear regression analysis of $(\hbar\omega\alpha)^2$ vs. $\hbar\omega$. Fig. 5 shows a bandgap of 5.60 eV for $SiN_{0.3}$ films. The non linear relation in the low energy region is due to surface light scattering.[10] The bandgap value we measured is smaller than that obtained by calculation (6.49 eV).[11] This is due to the non-stoichiometric composition of films. The extra silicon present in the films results in a subgap shoulder, which for amorphous silicon has been ascribed to dangling silicon bonds (trivalent silicon atoms). The subgap defect absorption levels are roughly two orders of magnitude larger in nitride films than that in amorphous silicon.[12] We suggest that Si-rich silicon nitride films have bandgaps smaller than stoichiometric or N-rich silicon nitride films. However, bandgap measurements reported by various researchers do not agree, moreover, there is at present no strict theory of light absorption in the amorphous state.[11]

When viewed under a microscope, the films were smooth over an area of 1 cm^2 - 4 cm^2. The "splashing effect" was also observed since no velocity filter was used in this work. It was also found that there was a threshold value of laser density for deposition of nitrogen-dominant films. The films grown in laser fluence smaller than 0.5J/cm^2 per pulse contain more oxygen than nitrogen.

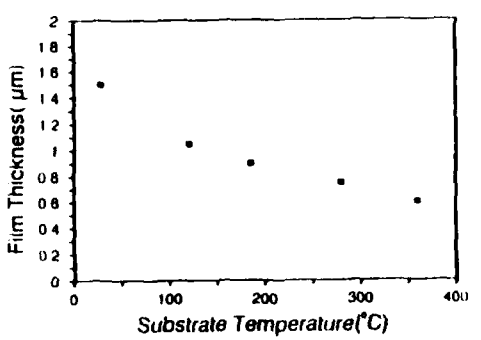

FIG.6. Relation between film thickness and substrate temperature after 15 min deposition with laser fluence of 6 J/cm^2 and a repetition rate of 5 Hz.

The film thicknesses were measured by a depth profilometer. The film grown at a substrate temperature of 210° C has a deposition rate of 2Å/pulse or 60nm/min. This deposition rate is extremely rapid in comparison to silicon nitride films formed by other deposition techniques (see, e.g, ref.1,3). Fig. 6 shows film thickness vs. substrate temperature after 15 min deposition at a laser fluence of 6J/cm^2 and a repetition rate of 5 Hz. It suggests that the deposition rate decreases when the substrate temperature increases. There may be a competition between evaporation of physically absorbed molecules on the surface and the formation of chemical bonds. Moreover, this type of competition may lead to the higher observed N/Si ratios at higher temperature, as some of the Si dangling bonds may be broken by thermal effects and then evaporate from the surface leaving the higher N/Si stoichiometric ratio. The high deposition rate is also an excellent promise for the application of silicon nitride films in microelectronics.

CONCLUSION

Thin silicon nitride films have been deposited by pulsed UV laser irradiation. These hydrogen-free films are non-stoichiometric and the chemical composition has been found to depend strongly on the deposition parameters. The optical properties of deposited films are equivalent to those of silicon nitride films grown by other techniques. The deposition rates are extremely rapid.

This work was supported by the NSF Grant No. HRD-9255378.

REFERENCE

1. S.L. Zhang, J.T. Wang, W. Kaplan, and M. Ostling, Thin Solid Films, **213**, 182 (1992).
2. C.H. Ling, C.Y. Kowk, and K. Prasad, J. Vac. Sci. Technol. A, **5**, 1874 (1987).
3. T. Ito, S. Hijiya, T. Nozaki, H. Arakawa, M. Shinoda, and Y. Fukukawa, J. Electrochem. Soc. **125**, 448 (1978).
4. S. Yokoyama, N. Kajihara, M. Hirose, Y. Osaka, T. Yoshihara, and H. Abe, J. Appl. Phys., **51**, 5470 (1980).
5. J.C. Barbour, H.J. Stein, O.A. Popov, M. Yoder, and C.A. Outten, J. Vac. Sci. Technol. A, **9**, 480 (1991).
6. A.C. Adams, *Plasma Deposited Films*, edited by J. Mort and F. Jansen (CRC Press, Inc., 1986), p. 134.
7. W.S. Lau, S.J. Fonash, and J. Kanicki, J. Appl. Phys. **66**, 2765 (1989).
8. S.W. Sun, P.J. Tobin, J. Weihmeir, and E. Reed, J. Electrochem. Soc., **134**, 1799 (1987).
9. E.A. Taft, J. Electrochem. Soc., **118**, 1341 (1971).
10. Kanekazu Seki, Xiangqun Xu, Hideo Okabe, Joan M. Frye, and Joshua B. Halpern, Appl. Phys. Lett., **60**, 2234 (1992).

11. V.I. Belyi, et al. *Silicon Nitride in Electronics*, (Elsevier Science Publishers, 1988), p. 154.
12. A. Iqbal, W.B. Jackson, C.C. Tsai, J.W. Allen, and C.W. Bates,Jr. J. Appl. Phys., **61**, 2947(1987).

Journal of Crystal Growth 00 (1993) JCG01792
North-Holland

S

CRYSTAL GROWTH

Laser-induced chemical vapor deposition of aluminum from trimethylaluminum: wavelength and temperature dependence

Kanekazu Seki [1], Joan M. Frye, Hideo Okabe and Joshua B. Halpern [2]

Department of Chemistry and Materials Science Research Center of Excellence, Howard University, Washington, DC 20059, USA

Received 29 January 1992; manuscript received in final form 2 April 1993

Aluminum films were produced [illegible]er-induced chemical vapor deposition (LICVD) from trimethylaluminum (TMA) using KrF (248 nm) and ArF (193 nm) exci[illegible]asers. Film growth was measured at substrate temperatures between 20 and 150°C. It is demonstrated that the deposition rate is governed by the mole fraction of gas phase TMA monomer in the region near the heated susceptor. At 248 nm, growth from the monomer was more than seven times as efficient as that from the dimer. LICVD from monomeric TMA at 248 nm was 3.5 times more efficient than at 193 nm. These experimental results suggest an improved LICVD method for aluminum deposition and deposition of aluminum containing materials such as GaAlAs.

1. Introduction

Trimethylaluminum (TMA) is of considerable industrial importance, and is commonly used as a precursor in chemical vapor deposition (CVD) of aluminum and other materials such as GaAlAs. TMA CVD usually involves pyrolysis. However, laser induced CVD has been investigated over the last decade [1–4] because it allows growth at lower substrate temperatures and thereby avoids interdiffusion of heteroatoms [5–7]. Since TMA is the simplest commercially available organometallic CVD aluminum source, studies have concentrated on this compound. Photoreaction mechanisms have been intensively discussed [2,3]. Detachment of methyl radicals appears to be the primary photochemical process in TMA photolysis as confirmed by Beuermann and Stuke [3]. Using picosecond laser mass spectroscopy they discovered that the primary products are excited dimethyl and monomethyl aluminum. Aluminum atoms are produced in a secondary reaction of dimethyl aluminum. Higashi [2] showed that the first excited state of the TMA was a weakly bound metastable state rather than a directly dissociative one by using laser-desorption time-of-flight mass spectroscopy and ab initio molecular orbital calculations.

Gas phase TMA is a dimer at room temperature which dissociates into monomers at higher temperatures [8,9]. The change in the UV spectrum between the dimer and monomer has been reported by this laboratory [10]. The absorption spectra shown in fig. 1 are taken from data in ref. [10] and remeasurements made by us. One observes that the monomer, which dominates at 125°C, has a strong, short-wavelength absorption followed by a weak, long-wavelength absorption. On the other hand, the dimer, dominant at 25°C, exhibits a strong short-wavelength absorption which does not extend beyond 220 nm. Most previous LICVD studies of TMA were done at room temperature; therefore, the photochemical reaction must have involved dimers and not monomers. Close examination shows that little work has been reported on the monomer deposition reaction. Further, no study has focused on

[1] Present address: ~~Chemical Kinetics and Thermodynamics Division, National Institute of Standards and Technology, Gaithersburgh, Maryland 20899, USA.~~

[2] To whom correspondence should be addressed.

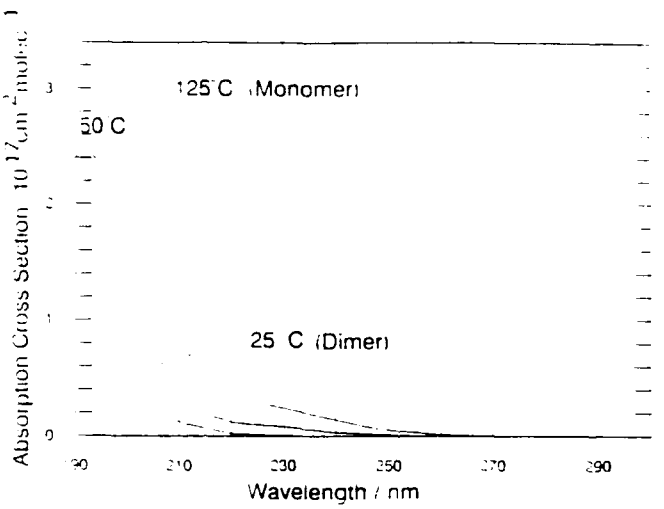

Fig. 1. Absorption cross section in cm² molecule⁻¹ (base e) for TMA in the 190–300 nm region at various temperatures: TMA is strongly dimerized at 25°C and has completely dissociated into monomers at 130°C.

differences in aluminum deposition following photolysis of the monomer or dimer.

This paper reports on aluminum deposition from TMA at various temperatures following excimer laser photolysis. Aluminum films deposited at a faster rate at 150°C than at 20°C following 248 and 193 nm LICVD of TMA. These results can be explained by reference to the monomer–dimer equilibrium and a knowledge of the absorption spectrum of both. LICVD at 248 nm near a warm substrate is shown to be a superior method.

2. Experimental procedure

Fig. 2 is a schematic diagram of the apparatus. TMA was vaporized by bubbling H_2 gas at a flow rate of 20 ml/min through liquid TMA. TMA–H_2 mixtures were introduced into a vacuum chamber whose base pressure was 10^{-2} Torr when evacuated by a two-stage mechanical pump. The total pressure of TMA and H_2 was about 7 Torr as monitored by a capacitance manometer. Irradiation was provided by a Questek excimer laser, operated with KrF or ArF. The pulse width was about 20 ns and the laser fluence per pulse was between 10 and 100 mJ/cm² at 10 Hz. The pulse was monitored by splitting off a known fraction of the beam and directing it to a power meter. The unfocused laser beam passed through a quartz window onto the substrate. Roughly 10^4 laser shots were used for each experiment.

The sample substrate attached to the metal susceptor and heated to temperatures as high as 200°C. The substrate was a 25 mm diameter, 1 mm thick fused silica plate which is transparent at 193 and 248 nm to minimize any possible laser

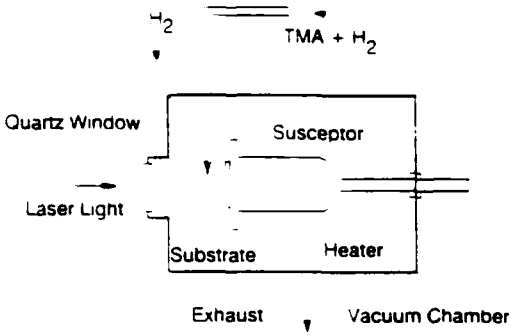

Fig. 2. Schematic diagram of the LICVD chamber for aluminum film growth from TMA.

heating. The temperature was measured by a thermocouple affixed directly to the substrate. The thickness of deposited aluminum was determined within ±5% using a depth profilemeter.

TMA was obtained commercially from Alfa Products with a stated purity of 99.999% on a metal basis (electronic grade). No detectable impurities were observed in the IR and UV spectra. The sample was used without further purification.

3. Results

Aluminum films were produced by LICVD from TMA at various temperatures between 20 and 150°C following KrF (248 nm) and ArF (193 nm) irradiation. Auger electron spectra were measured for samples deposited at 150°C at 193 and 248 nm. Ar ion sputtering was used to remove any surface contamination. The films contain 95% Al, 4% O, and < 1% C. No difference was observed in atomic concentration of the films produced by 193 and 248 nm excitation.

Fig. 3 shows the thickness of aluminum films grown by 248 nm KrF LICVD as a function of substrate temperature. The partial pressure of the TMA was 1 Torr. The film produced at 20°C was visible to the naked eye, but it was too thin to be measured by the profilometer (< 0.05 μm). Below 100°C the thickness rises in proportion to the temperature. Above 130°C saturation occurs. No aluminum deposition was observed in the absence of laser irradiation even at 150°C. The ordinate on the right side of the figure gives the mole fraction of monomer present at various pressures.

The 193 nm laser quickly deposited aluminum on the inside surface of the cell window, attenuating the laser light before it reached the substrate. To avoid this, additional hydrogen was injected around the window. Nevertheless, aluminum growth on the substrate following 193 nm irradiation was small, below 0.1 μm. The reproducibility of film growth at 193 nm was also poor. Both of these effects can be explained by the absorption of light in the vacuum chamber. At 193 nm, light is absorbed near the window of the reaction chamber as described above, and in the volume between the window and the substrate.

In order to compare growth of the monomer and dimer at 193 and 248 nm, films were grown

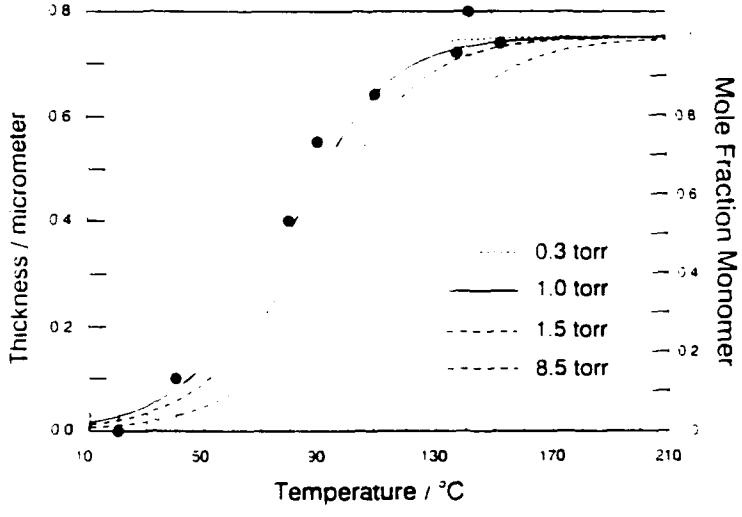

Fig. 3. The left ordinate and the data points show the thickness of aluminum films produced from LICVD of TMA using 248 nm laser irradiation as a function of substrate temperature. The right ordinate and the lines show the mole percent of monomer as a function of substrate temperature and pressure.

Table 1
Relative quantum yields of Al films grown by LICVD

Wavelength (nm)	State	Temperature (°C)	Deposition rate (nm/min)	σ (10^{-18} molecules cm^{-2})	Relative quantum yield
193	Monomer	20 ± 2	1200	31.0	1.00
	Dimer	25 ± 2	260	20.0	0.34
248	Monomer	20 ± 2	110	1.8	3.50
	Dimer	25 ± 2	-	0.1	< 0.50

on the inside of the vacuum cell window. Growth from the monomer was carried out by warming the outside of the window with a heat gun. A thermocouple, attached to the inside of the window ensured that the window surface was hot enough to promote the formation of TMA monomers in the cell. Results are summarized in table 1. Yields were normalized for the number of photons absorbed using the cross-sections of Okabe, Emadi-Babaki and McCrary [10]. The relative quantum yield refers to the film thickness for an equivalent number of laser shots at 5 mJ/cm^2 · pulse and 10 Hz. The yield for the 193 monomer is arbitrarily taken as the reference.

Any Al deposited on the window attenuates the laser light. Therefore, the deposition rate at any point in the process would depend to some extent on the thickness deposited previously. In this set of experiments, where growth was observed, the growth continued until the thickness of aluminum deposited reached about 0.3 μm. In any case, this error underestimates the relative yield of deposition at the most efficient wavelengths and temperatures and overestimates the yield when the efficiency is low.

Growth from dimers is seen to be less efficient both at 193 and at 248 nm. At 248 nm, the film was actually too thin to measure with the profilemeter. The relative yield for growth from the dimer would thus be an upper limit. On a per photon absorbed basis, growth from the monomer at 248 is 3.5 times as efficient as that at 193 nm.

4. Discussion

The experimental results in fig. 3 can be explained by reference to the equilibrium between the TMA dimer and the monomer and the photoabsorption profiles. The degree of dissociation of TMA dimer into monomer, α, is given by [8,9]

$$\alpha = \left[K_p/(K_p + 4P/760) \right]^{1/2}, \quad (1)$$

where the equilibrium constant K_p is [11]

$$\log_{10} K_p(\text{atm}) = 9.4395 - 4457.9/T. \quad (2)$$

P_{max}, the vapor pressure of TMA, is [8]

$$\log_{10} P_{max}(\text{Torr}) = -2104/T + 8.152. \quad (3)$$

and T is the absolute temperature. The fraction of monomer calculated using eqs. (1) and (2) depends on the temperature and the partial pressure of TMA in the cell. In fig. 3, one sees that more monomer is formed as the temperature increases or the TMA partial pressure decreases. The partial pressure of TMA in the reaction chamber during film growth was about 1 Torr. At 20°C and 1 Torr, TMA is substantially dimerized; however, the monomer is dominant at 150°C.

The temperature distribution in the reaction chamber was not homogeneous because of the flow of gas, as shown in fig. 2. Only gas near the substrate was warmed by the heater. The rest remained at room temperature. That is, if the substrate is maintained at 150°C, only the TMA molecules near the substrate were heated and dissociated into the monomer. The rest remained as dimers.

Fig. 3 shows that aluminum deposition at 248 nm correlates with the mole fraction of monomer near the substrate. This, however, does not necessarily mean that the reactivity of dimer is low. The monomer absorption at 248 nm is 0.8×10^{-18} cm^{-2} molecule^{-1} and that of the dimer is 0.1×10^{-18} cm^{-2} molecule^{-1} [10]. According to eq. (1), the mole fractions of monomer at 20°C and 150°C are 2% and 97%, respectively, at 1.5 Torr. If, at 248 nm, the dimer and monomer aluminum deposition efficiencies were equal, the ratio of film thickness produced would be 1 to 8, the ratio of the absorption cross section of the dimer and

the monomer. The observed value is, however, at least 1 to 15, as seen in fig. 3, where the instrumental limit of 0.05 μm has been assumed as the thickness for the films deposited at 20°C. Referring to table 1, the lower limit to this efficiency ratio is 1 : 7 when the different absorption coefficients are taken into account.

The difference between the photochemical processes involving dimer and monomer can be discussed in terms of their electronic structure. Beuermann and Stuke [3] reported that the main products of low pressure monomer photolysis at 248 nm were aluminum atoms. They suggested the following mechanisms for monomer photolysis in the UV region (190–300 nm):

$$Al(CH_3)_3 + h\nu \rightarrow Al(CH_3)_2^* + CH_3, \quad (A),$$

$$Al(CH_3)_2^* \rightarrow Al + C_2H_6, \quad (B),$$

$$Al(CH_3)_3 + h\nu \rightarrow AlCH_3 + 2\,CH_3, \quad (C),$$

where $Al(CH_3)_2^*$ is a metastable radical. Their data showed that process (C) was the main channel below 210 nm and process (A) followed by process (B) was dominant above 230 nm. Therefore, aluminum atoms are the end product of monomer photolysis at 248 nm, which would suggest that aluminum deposition from the monomer by photolysis at 248 nm is effective. Motooka et al. [1] studied dimer photolysis at 193 and 248 nm and suggested that the photoexcited dimer reacted by separating into the monomer. Therefore, dimer photolysis would not be as effective as monomer photolysis, because aluminum generation from the dimer requires absorption of an additional photon to produce an aluminum atom. Both of these reports support the results presented here.

The dimer forms when two methyl groups, one from each TMA monomer, are shared between the two aluminum atoms forming a bridge structure. The overall symmetry is C_{2v}. The monomer is planar with D_{3h} symmetry. The monomer absorption above 210 nm was taken as an e′ to a_2'' or a_2', to a_2'' transition by Okabe et al. [10]. The e′, a_2'', and a_2', refer respectively to a degenerate p orbital of the aluminum and carbon atoms, an unoccupied p_z orbital of the aluminum atom, and a lone pair p orbital located predominantly on a carbon atom. These transitions are forbidden and therefore weak.

Both the dimer and the monomer have strong Rydberg bands at 193 nm. Deposition from dimers is inherently less efficient because of the necessity of breaking the additional dimer bonds to form aluminum. The weak dimer absorption at 248 nm is in the tail of the Rydberg absorption and of the same nature as the dimer absorption at 193 nm.

These experimental results show that the reaction path from a_2'' is more effective than that from the Rydberg states for aluminum deposition by LICVD from TMA.

Not only LICVD, but all light activated CVD processes share a common disadvantage. It is difficult to concentrate the reactive chemical species around the substrate in order to achieve rapid film growth because much of the incident light does not reach the region near the substrate, but is absorbed by molecules lying between the substrate and the window. For example, if one reduced the partial TMA pressure in order to increase the light flux at the substrate, the number of TMA molecules near the substrate, and therefore the efficiency of Al production, would decrease proportionally. Even if the pressure was reduced, the TMA would absorb throughout the laser path, not only near the substrate. In the method demonstrated here, the substrate was heated to 130°C and illuminated with 248 nm light. Because TMA is almost completely dimerized except near the substrate, the 248 nm light was not absorbed in the middle of the cell. Only the monomeric TMA near the heated substrate absorbed 248 nm light. This produced aluminum atoms only in the neighborhood of the substrate, where they effectively formed a film. Furthermore, the yield of aluminum per 248 nm photon absorbed by the monomer is substantially higher than that from the dimer and higher than that formed from the monomer at 193 nm. Thus 248 nm photolysis of TMA near a warm substrate is a superior LICVD method for aluminum film growth at relatively low temperatures ($100 < T < 150$°C).

5. Conclusion

Aluminum films have been grown by LICVD from TMA using KrF (248 nm) and ArF (193 nm) excimer lasers. The efficiency of aluminum deposition has been measured at various substrate temperatures between 20 and 150°C. The efficiency depends strongly on the temperature for 248 nm excitation. The temperature dependence is less pronounced for 193 nm excitation. This is explained by the equilibrium between TMA dimers and monomers and their absorption spectra. At higher temperatures, the equilibrium shifts to the monomer and above 130°C TMA exists as a pure monomer. Since only the monomer absorbs 248 nm light, the TMA photoreaction is proportional to rising temperature, as is aluminum deposition. While both the dimer and monomer have strong Rydberg absorption at 193 nm, deposition from the dimer requires absorption of two photons and is slower than deposition from the monomer. Moreover, deposition from the monomer is three to four times as efficient at 248 nm than at 193 nm. Finally, an improved method for aluminum deposition from TMA at relatively low temperature conditions has been demonstrated, using 248 nm photolysis of TMA.

Acknowledgements

This work was supported by the US Air force Grant FQ8671-89-01458 2306/B1. The authors wish to thank D. Arugu for the Auger measurements.

References

[1] T. Motooka, S. Gorbatkin, D. Lubben, and J.E. Greene, J. Appl. Phys. 58 (1985) 4394
[2] G.S. Higashi, J. Chem.Phys. 88 (1988) 422.
[3] Th. Beuermann and M. Stuke, Chem. Phys. Letters 178 (1991) 197.
[4] S.A. Mitchell and P.A. Hackett, J. Chem. Phys. 79 (1983) 4815; Chem. Phys. Letters 107 (1984) 508.
[5] D.J. Ehrlich, R.H. Osgood, Jr. and T.F. Deutsch, IEEE J. Quantum Electron. QE-6 (1980) 1233.
[6] D.J. Ehrlich and J.Y. Tsao, J. Vacuum Sci. Technol. B 1 (1983) 969.
[7] R.M. Osgood and T.F. Deutsch, Science 227 (1985) 709
[8] A.M. Laubengayer and W.F. Gilliam, J. Am. Chem. Soc. 63 (1941) 477.
[9] M.B. Smith, J. Organometal. Chem. 46 (1972) 31.
[10] H. Okabe, M.K. Emadi-Babaki and V.R. McCrary, J. Appl. Phys. 69 (1991) 1730.
[11] A. Amirav, A. Penner and R. Bersohn, J. Chem. Phys. 90 (1989) 5232.